

Conformational Analysis of Environmental Agents: Use of X-Ray Crystallographic Data to Determine Molecular Reactivity

by Vivian Cody*

This paper explores the use of crystallographic techniques as an aid in understanding the molecular reactivities of a number of agents that are of concern to pharmacologists and toxicologists. The selected examples demonstrate the role of structural data in the determination of absolute configuration, conformational flexibility and active-site topology for a reactive species. For example, the role of absolute stereochemistry in understanding synthetic pyrethroid structure-activity relationships is shown from analysis of their crystal structures; conformational flexibility among DDT analogues, and the importance of conformational and electronic properties in phenylalkanoic acid herbicides are shown from systematic analysis of their crystal structures; and interpretation of active-site stereochemistry is made by study of computer modeling of enzyme inhibitors in the active sites of related protein crystal structures. Thus, the observed patterns in conformational flexibility and their resultant effects on substrate pharmacological profile can be interpreted in understanding the molecular level events that influence biological reactivity.

Introduction

Many strategies have been employed to understand the molecular reactivities of small molecule substrates acting at their target sites. The premise underlying the development of structure-activity relationships is that the correlations that exist between molecular structure (or molecular shape) and observed biological responses are the result of these substrates (hormones, drugs, metabolites, agonists, antagonists, etc.) interacting with their macromolecular target sites (receptors, enzymes, binding proteins, etc.). Thus, interaction with the target molecule not only depends upon substrate chemical constitution, including such properties as charge, polarity, and hydrophobic character, but also on the geometric disposition of key moieties. Therefore, a detailed knowledge of molecular structure is fundamental to the understanding of structure-activity relationships.

An X-ray crystal structure determination provides a detailed picture of the contents of a crystal lattice at the atomic level and will uniquely define the three-dimensional conformation of a molecule from its atomic positions. Provided one has a reasonably good quality crystal, these parameters can provide an accurate description of the intramolecular geometry (bond lengths, angles, and torsion angles to within ± 0.0003 – 0.005 Å and ± 0.1 – 0.4°), and also describe intermolecular in-

teractions such as hydrogen bonding and charge-transfer between molecules. Moreover, the presence of anomalously scattering atoms in the structure (e.g., halogens) will permit the absolute configuration of all chiral centers in the molecule to be defined. Also, data from neutron diffraction experiments permit accurate location of hydrogen atoms in the structure. Finally, high resolution X-ray diffraction studies can describe the electron density distribution within the bonding atoms from charge-density studies.

Crystallographic observation of the substrate, target, and target-substrate complex can provide the most reliable description of these molecular interactions, as well as provide information concerning conformational preferences in flexible molecules. However, in general, little is known of the target site, and the stereochemical requirements of the substrate-target interactions are often poorly understood. For this reason, target-site topology has been deduced from comparisons of structural data (solid state, solution, or isolated molecule) for a series of compounds that bind to the target site and elicit varying degrees of activity.

However, to understand how substrate molecular conformation can influence observed reactivity, it is necessary to understand the factors that control conformational properties. While there are a number of terms contributing to the total lattice energy in organic crystals, only a few of these intermolecular forces are large enough to influence molecular conformation. The prin-

*Medical Foundation of Buffalo Inc., 73 High St., Buffalo, NY 14203.

cial terms considered in calculating the energetics of conformational change include van der Waals forces, hydrogen bonding, charge-transfer, and electrostatic energies.

While the crystal structure of a substrate will provide information concerning its preferred conformation in a particular environment, it provides no information concerning the energy differences between conformations and the energy barriers that separate them. Therefore, by comparing the crystallographically observed conformation with that (1) in solution, (2) in the free state, (3) in different polymorphs, and (4) of different conformers in the same crystal, the relative influence of these intermolecular forces on molecular conformation can be investigated. Also, by analyzing the crystal structures of a number of closely related molecules, one can look for patterns in the consistency of their structural features, and credence can be given to trends which may not be statistically significant by themselves.

Thus, X-ray crystallographic techniques permit accurate identification of the chemical constituents, definition of the absolute stereochemistry, and determination of the range of conformational flexibility of substrate molecules. Also, patterns in conformational flexibility and their resultant effects on substrate pharmacological profile can be of importance in understanding the molecular level events that influence biological reactivity.

This paper will explore the use of crystallographic techniques as an aid in understanding the molecular reactivity of a number of systems that are of concern to pharmacologists and toxicologists. In choosing these examples, the aim is not to provide an exhaustive review of the literature, but to illustrate, with selected examples, the role of crystallographic data in the determination of configuration, conformation, or active-site topology of a reactive species.

Structure-Activity Relationships

Environmental Agents

Given in sufficient doses, most chemicals are toxic poisons. Even the use of chemicals for their intended purpose can lead to problems of contamination and disposal. Also, a growing awareness and concern over the use of chemical agents that are either deliberately (e.g., pesticides) or inadvertently (e.g., pollutants) added to the environment have led to renewed efforts to understand their degradation and translocation in the environment, as well as their metabolism and effect on other species.

The release into the atmosphere of polycyclic aromatic hydrocarbons that result from incomplete combustion of fossil fuels and vegetation has caused concern since many of these environmental pollutants are carcinogenic. Also, the extensive use of halogenated aromatic compounds in many commercial products has made their disposal an environmental hazard because of their high chemical stability and lipophilicity which lead to

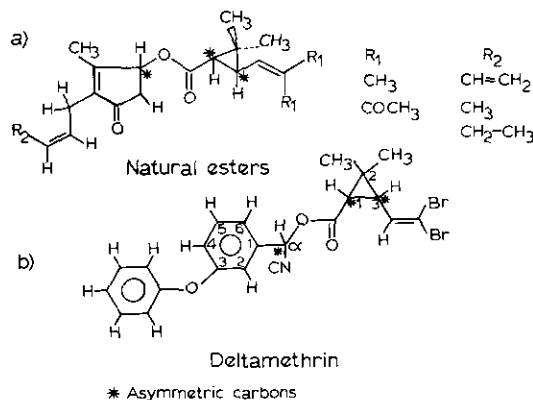


FIGURE 1. (a) Structures of natural pyrethrin esters and (b) potent synthetic pyrethrin analog showing asymmetric carbons and numbering.

long-term bioaccumulation (1,2). Pesticides are those agents that are purposely, and often routinely, added to the environment for the purpose of killing some form of life; plant (herbicides) or animal (insecticides).

Pyrethroid Insecticides. Synthetic pyrethroid insecticides are photostable analogs of the naturally occurring pyrethrin esters (Fig. 1) and have low mammalian toxicity, short persistence in the environment, and elicit rapid insect paralysis (3). The most potent pyrethrine analogs can have eight possible isomers formed by combinations of configurations about the three asymmetric carbons in the structure (Fig. 1b). Structure-function data show that the most active pyrethroid compounds are cyclopropane carboxylic acid esters with two methyl groups on C-2 and an unsaturated side chain on C-3 which is oriented *cis* to the ester group (Fig. 1) in synthetic pyrethroids and *trans* in the natural esters (3). Substitution of these groups results in a great loss of activity. These characteristics suggest the importance of molecular shape in activity. X-ray crystallographic analyses were carried out to determine reliable structural information concerning absolute stereochemistry, molecular dimensions, and conformation (4-7).

The absolute configuration of the most potent insecticide (Fig. 2a) in this series is (α S) *cis* (1R,3R), as determined from its crystal structure (5). The structural data for three other analogs (5-7) show that although the molecule is flexible (Fig. 2), there are regions with conformational similarities. All the structures were resolved into their optical antipodes except that of Figure 2c, which crystallized as a racemic mixture and is shown as the (α S) *trans* (1S,3R) isomer.

In this series, the conformational influence of two substituents—benzylic cyano and vinyl halogens—were studied. Those structures without the cyano group are less active and, because their crystal structures are isomorphous (Fig. 2b,d), there are no conformational differences. When there is no α -cyano substitution, and thus a loss of a chiral center, the ester oxygen is coplanar with the phenyl ring, while in the two cyano compounds the ester bond is nearly perpendicular. In addition, the two cyano analogs have different stereochemistries at

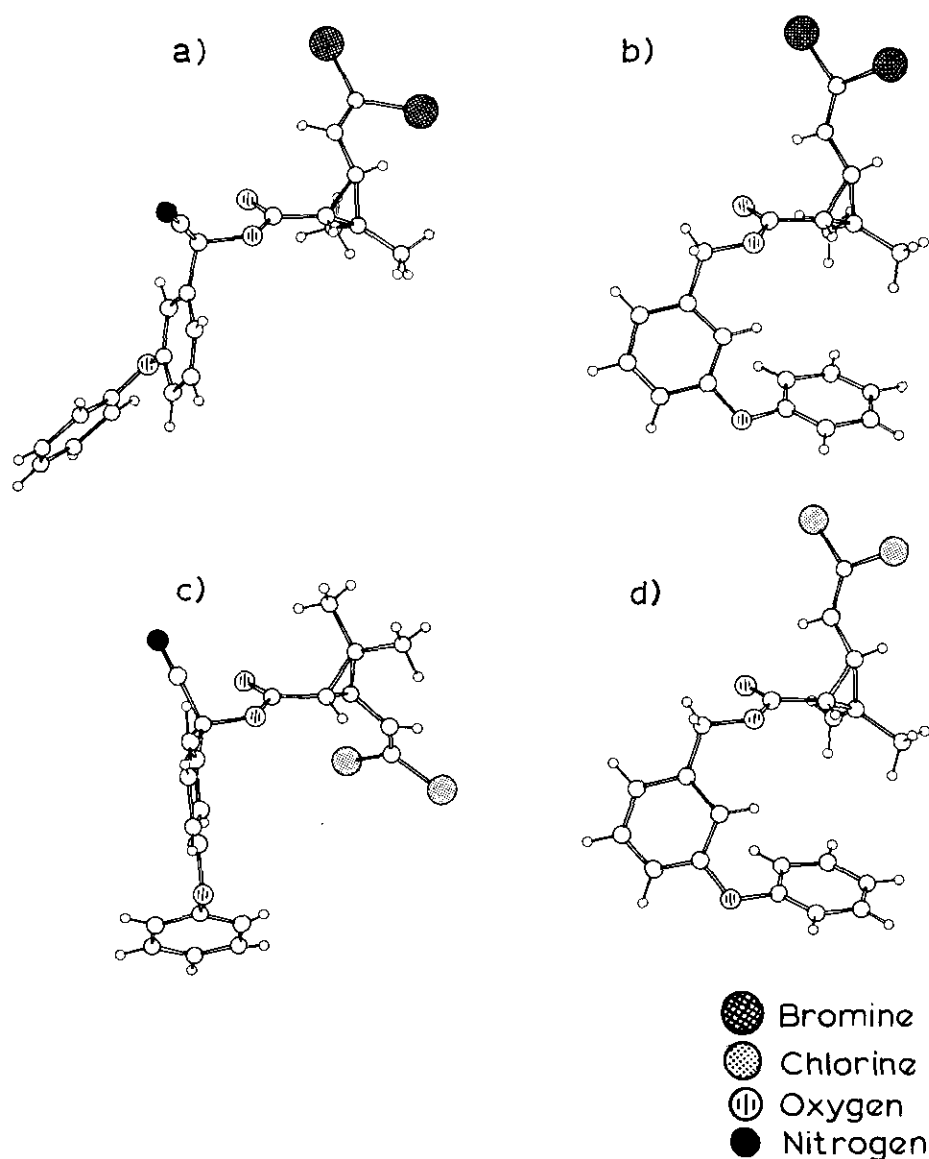


FIGURE 2. Crystallographic conformations of four synthetic pyrethrin analogs: (a) α -cyano *cis*-3-(2,2-dibromovinyl) analog (5); (b) *cis*-3-(2,2-dibromovinyl) analog (6); (c) (1*R*,*trans*)-3-(2,2-dichlorovinyl) analog (7); (d) *cis*-3-(2,2-dichlorovinyl) analog (6).

C-1. The conformation of the diphenyl ether moiety in these structures is either twist or antiskew (8,9), as defined by the torsion angles about the ether oxygen. The net effect of these different diphenyl ether conformations is to change the overall shape of the molecule. In the structure without the cyano substituent, the diphenyl ether conformation is twist and the outer phenyl ring folds back toward the gem dimethyl of the cyclopropyl ring (Fig. 2*b,d*). In the active isomer (Fig. 2*a*), the diphenyl ether conformation is twist and the molecule is more extended. The racemic structure (Figure 2*c*) has the opposite chiral stereochemistry at C-1 from that of Figure 2*a*, and further has an antiskew diphenyl ether conformation. This places the vinyl chlorine atoms toward the center of the inner ring.

Preferred conformations computed by theoretical calculations (10) were carried out for these pyrethroids

and show that the minimum energy conformation corresponds to that observed in the crystal structure. These calculations also indicate that there is restricted rotation of the vinyl group, resulting in a preferred conformation that is also observed in solution (10) and in the crystal structure (Fig. 2*d*). Although these calculations show no preferred conformation for rotation about the alpha carbon, the extended form is observed both in solution and in the crystal structure.

Therefore, these structural studies have delineated the absolute configuration about the critical chiral centers and have shed light on the conformational influence of active group substitution to the overall molecular shape. These data are also consistent with solution studies (10) showing that the proximity of the cyano and ester groups is important for activity.

Organochlorine Insecticides. The organochlorine

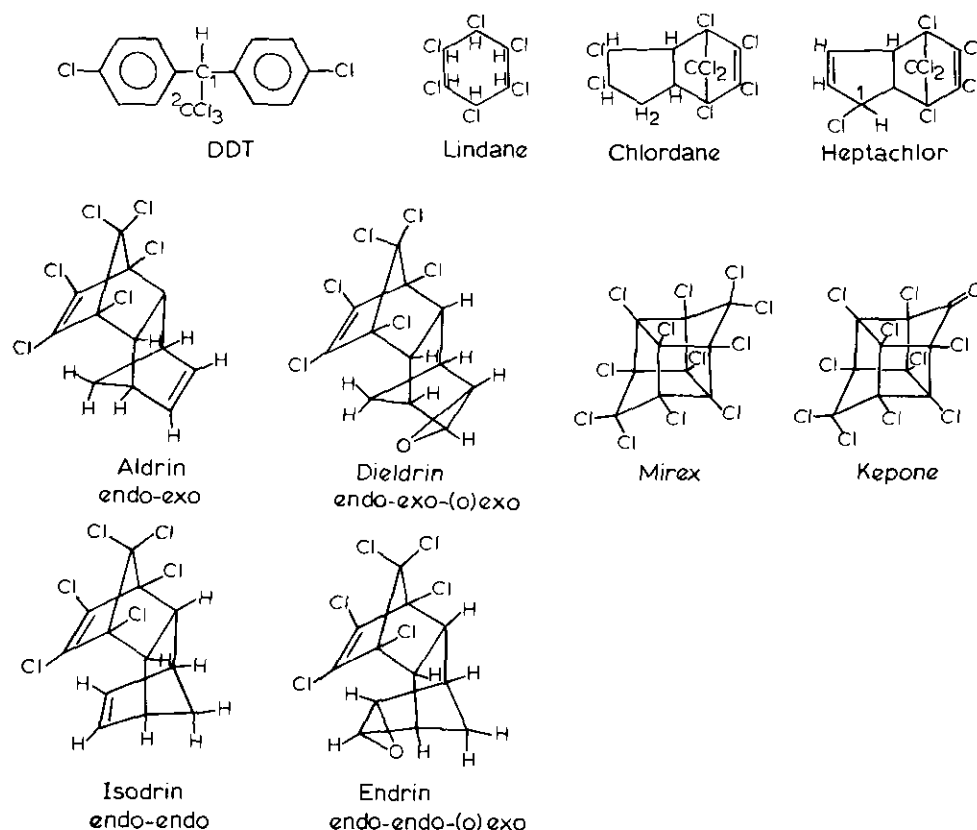


FIGURE 3. Organochlorine insecticide classes which all act as neuropoisons, although their mechanisms of action are presumed at different sites.

insecticides include the chlorinated ethane derivatives of which DDT is the best known example. Other classes include the cyclodienes such as chlordane, aldrin, and endrin, which are chloromethano-bridged cyclic carbon compounds; the hexachlorocyclohexanes such as lindane; and the fused chlorocyclopentanes such as mirex and kepone (Fig. 3). While all of these classes act as neuropoisons, their mechanism or site of action is not yet clearly understood (1).

Toxicological studies indicate that DDT alters the transport of Na^+ and K^+ ions across the membranes of nerve axons by producing a repetitive discharge of the insect nervous system. Its mechanism of action is thought to involve a stereospecific fit into nerve membrane-pore channels and the formation of charge-transfer complexes with constituents in the nerve fibers (11-13). In this general receptor model, a constraint is placed upon the conformation of the two phenyl rings such that their symmetrical dipoles are sterically fixed relative to the trihalomethyl bridging group. This fixes the two phenyl rings in a "butterfly" conformation, e.g., with both rings perpendicular to the plane of the bridging atoms.

These structure-activity data show that several features of the DDT molecule are important to its insecticidal properties. For example, substitutions larger than chlorine on the bridge ethane C-1 atom produce inactive analogues; chlorination of the bridge head carbon results in a twisted diphenyl ring conformation and loss of activity; and an ethylene bridging unit causes loss in ac-

tivity, presumably because the bridge angle opens to 120° and changes the orientation of the *p,p'*-chloro groups (12). Therefore, the important conformational features for active DDT analogs include (1) the rotation of the phenyl rings about the bridge atom, (2) the nature of the bridge substituent, and (3) the nature and position of the phenyl ring substituents.

To investigate the molecular mechanism of DDT action, the crystal structures of several active DDT analogs were undertaken (13-21). As illustrated (Figs. 4 and 5), the overall conformation of the diphenyl rings is variable but similar to the proposed model. Since these molecules crystallize in centrosymmetric space groups, there are two mirror-image conformations possible. The absolute configuration has been determined for only one DDT analog; (-) *o,p'*-DDT (15), and all other structures have been made consistent with this enantiomorph for the purpose of comparison.

The proposed active DDT conformation has two phenyl rings open and facing each other (e.g., butterfly) with the bridging torsion parameters near 90° for both angles. These structural studies show (Fig. 5) that, while there is a broad range of values observed for these parameters, they all fall within the same quadrant of conformational space. The most toxic analogs are clustered close together (e.g., Nos. 1-4), while those that are moderately active (e.g., Nos. 7, 13-15) are more broadly grouped. This group also includes the active halogen-free analogs (Nos. 13, 14). The inactive analogs

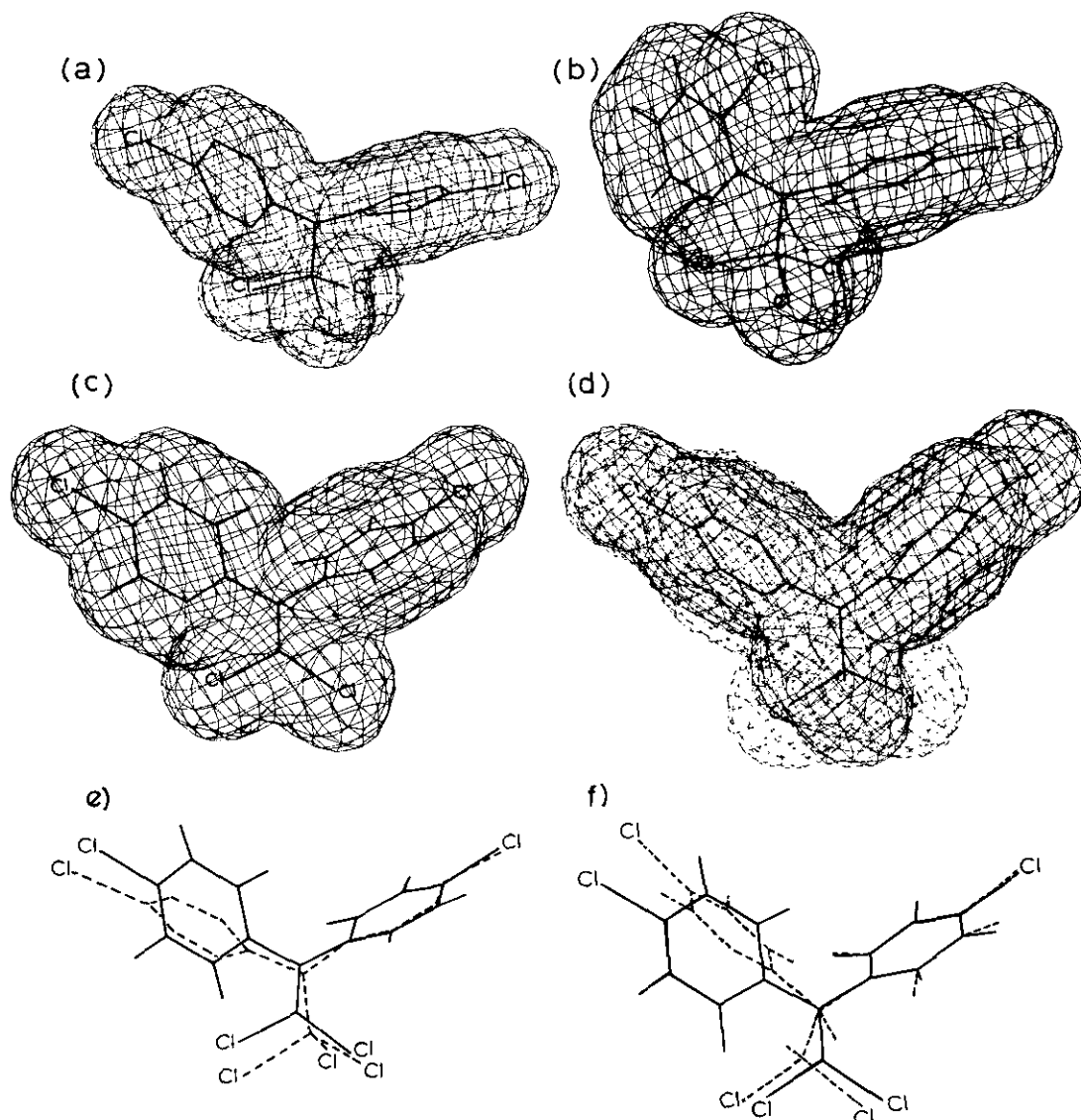


FIGURE 4. Molecular conformation of DDT analogs: (a) *p,p'*-DDT (14) with van der Waals surface, highly active; (b) *o,p'*-DDT (15) with van der Waals surface, inactive; (c) *p,p'*-DDE (17) with van der Waals surface, inactive; (d) overlap of (c) and the dichloromethyl analog (17) (dashed surface) illustrating the larger volume of the active analog; (e) overlap of (a) and (c); (f) overlap of (c) and (d). The conformational parameters of these compounds are points 1, 2, 8, and 10 of Fig. 5, respectively.

(Nos. 8,9,11,12) are located at the extremes of this conformational space. As illustrated (Fig. 6), there is a large conformational difference between active 2,2-dichloromethyl analog (No. 10) and its inactive dichloroethylene analog (Nos. 8,9). The bridging angle in the ethylene structure is 118° and 109° in the methyl compound, and there is a difference in the volume occupied by these bridging groups that appears to be important for activity. A similar difference is noted for the inactive acid metabolite, *p,p'*-DDA (Nos. 11,12) which also occupies a smaller volume and has electronic properties similar to those of the ethylene compound. The importance of these properties is further reflected in the moderate activity of the propyl bridge analog (No. 13), which is halogen-free.

These studies have defined the molecular size and shape necessary to elicit insecticidal activity and have shown that, as the aromatic character of the bridging

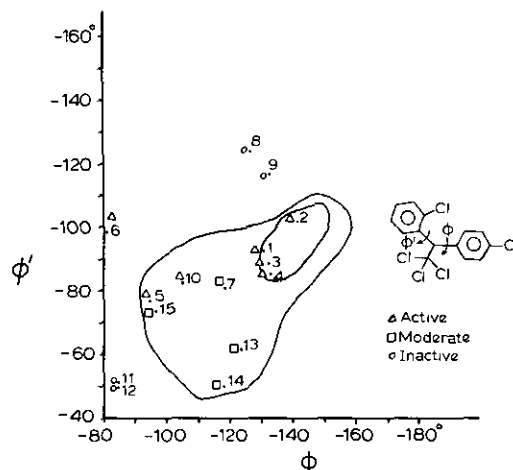


FIGURE 5. Plot of DDT halomethyl bridge torsion angles as defined in the diagram (13-21).

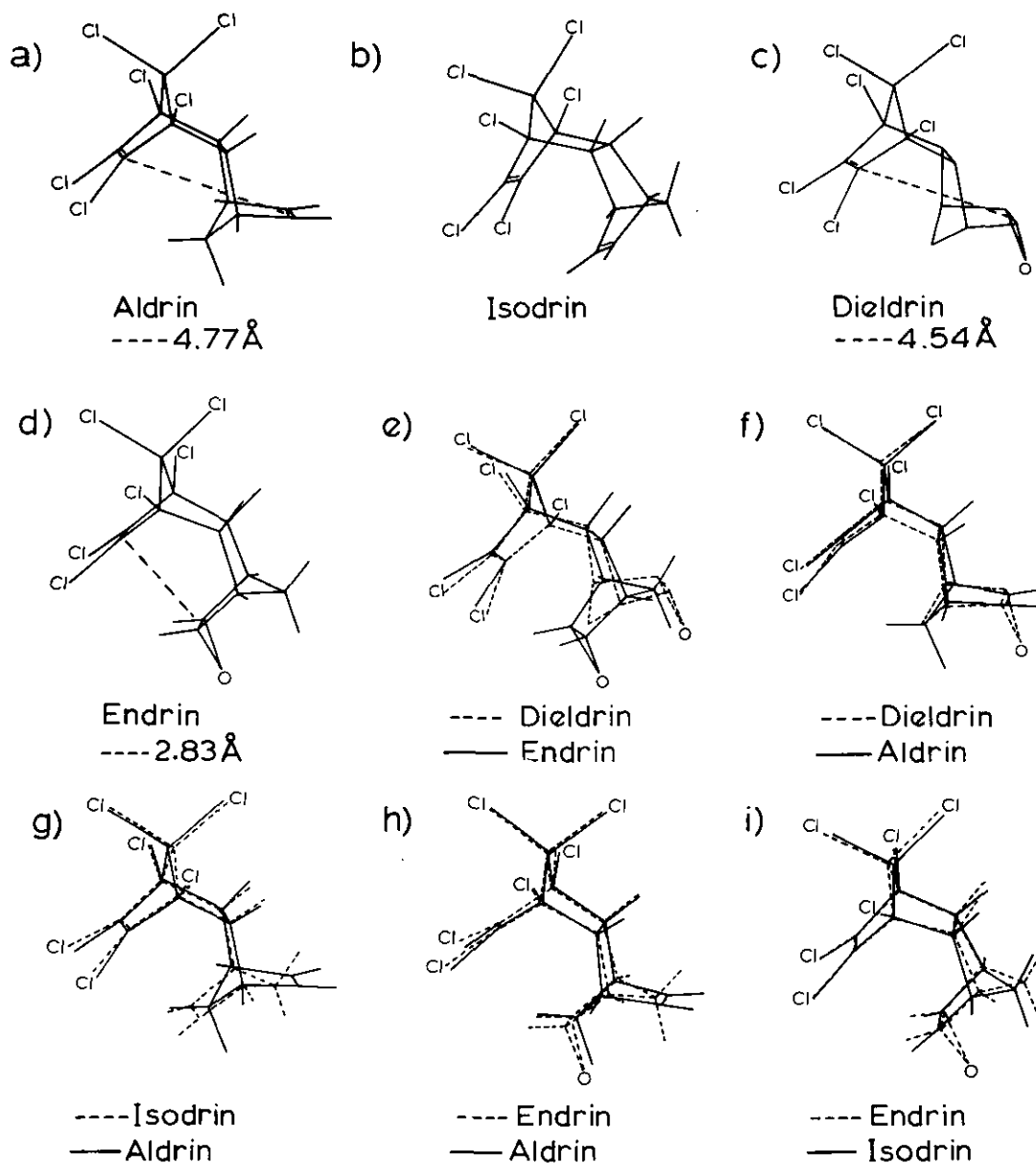


FIGURE 6. Crystallographic conformations of organochlorine insecticides: (a) aldrin (23); (b) isodrin (24); (c) endrin (23); (d) dieldrin (25), illustrating their *endo-exo* configurations and oxo formation; (e-g) show the overlap of these respective structures. The distance between the electronegative centers are also illustrated.

unit increases (e.g., Figs. 4c,d), its toxicity decreases. Furthermore, these data show that an isostructural unit of size similar to that of the trichlormethyl group can function to sterically fix the conformation of the diphenyl rings and that chloro substitution of the bridge is not necessary.

The chlorinated cyclodienes (Fig. 3) are wide-spectrum insecticides produced by a Diels-Alder reaction between the cyclic diene, hexachlorocyclopentadiene, and an olefin. The insecticidal activity of the resulting adducts depends on the nature and complexity of the dienophile and its substituents. Structure-activity data illustrate that the geometrical patterns of these compounds have an important bearing on their insecticidal

properties (22). These data further suggest that the structural features required for optimal insecticidal activity include the presence of two electronegative centers positioned within a narrow range of distance and direction from each other and with a specific orientation with respect to the dichloromethano bridge of the cyclodiene compound. It has been shown that the cyclodiene epoxides are metabolically active; thus those compounds that do not form epoxides have little or no toxicity (22).

To understand the stereochemical nature of these insecticides, crystal structure analyses of the most active cyclodienes have been investigated (22-28). The most toxic compounds are a family of hexachlorodimethano-

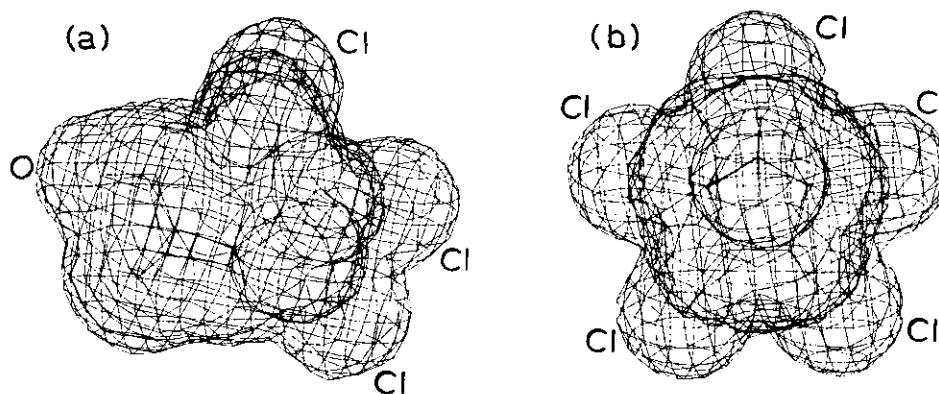


FIGURE 7. van der Waals surface for endrin (23) viewed (a) parallel to the distance shown in Fig. 6, and (b) perpendicular to this line.

naphthalenes, e.g., aldrin (Fig. 3). While there are four different geometric configurations possible for these compounds, structural data show that only two isomers are observed: *endo-exo* aldrin (23) and *endo-endo* isodrin (24) and endrin (23) (Fig. 6).*

The importance of molecular shape in relation to insecticidal activity is illustrated by the comparison of *endo-exo*-(O)*exo* dieldrin (25) with its *endo-endo*-(O)*exo* isomer, endrin (24) (Fig. 6), which has lower toxicity (22). This indicates that the spatial orientation of the electronegative oxygen in dieldrin is critical for toxicity. The overall shape of dieldrin is cylindrical with the chlorines describing the maximum circumference of the cylinder. Dieldrin is more elongated than its *endo-endo* isomer endrin (Fig. 7). The distance between the two electronegative centers (midpoint of the double bond to the midpoint of the C-C bond of the oxo ring) is also shown for these molecules (Fig. 6). These data suggest that the active site recognizes only a narrow range of values for these compounds.

Another family of active dienes, the hexachloromethanoindenes, e.g., heptachlor (Fig. 3), show increased toxicity with addition of a chlorine in the 1-position. The structure of the heptachlor (27) and its epoxide (28) have been carried out and show the epoxide is *exo*, an important configuration for the high toxicity of this class of compounds (22).

Therefore, these structural studies have confirmed the stereochemical assignment of the active cyclodienes and show that the relative orientation of the electronegative groups is critical for their insecticidal activity.

Herbicides. The halogenated phenoxyalkanoic acids selectively kill broad-leaved plants by stimulating excessive and disorganized growth, thus acting as auxins or plant hormone herbicides (1). These compounds also

demonstrate molecular engineering techniques by taking advantage of species metabolic differences to create species selective herbicides. The most potent herbicides in this class are 2,4-dichlorophenoxyacetic acid (2,4-D), 2,3,5-trichlorophenoxyacetic acid (2,4,5-T), and 4-chloro-2-methylphenoxyacetic acid (MCPA) (Fig. 8). The corresponding 2-methyl-2-phenoxypropionic acids are inactive as herbicides, but do possess antilipolytic and antihypocholesterolemic activity (1).

Structure-activity data indicate stringent stereospecific requirements for recognition by a receptor in order to elicit herbicidal activity (29,30). Phenoxyalkanoic acids with only phenyl ring substituents at either the 2,4, or 5 position (or in all of them) are active, whereas symmetrically substituted phenyl ring compounds are not. Also, those chlorophenyl analogs with a methyl at the acetic acid C-1 position are active, but not those with a dimethyl substitution. The influence of phenyl ring substitution and side chain substitution is reflected by the activity and inactivity of the pairs of compounds *p*-chlorophenylacetic acid (No. 5, Fig. 8) and phenylacetic acid (No. 1) and 2,4-D (No. 6) and its 2,2-dimethyl side chain analog (No. 7). These data also show that an ether link is essential for auxin activity and that when there is an asymmetric carbon in the side chain, the D-isomers are more potent than the L isomers (29,30). Based on these structure-activity relationships, a three-point contact receptor model was proposed which required the proper orientation of the acid side chain carboxyl group, the α -hydrogen and phenyl ring with appropriate electronegative characteristics (29,30).

Crystallographic analyses of phenoxyalkanoic acids were carried out to determine the conformational properties of this class of compounds and to elucidate the specific stereochemical features that could explain their herbicidal activity (31,32). These data show striking conformational similarities among these structures and indicate that there is a distortion of the *exo*-C-1 acetic acid bond angles and also of the central atom of the acid function (31). In addition, the ether bond angle is near 118°, and the bridging bond distances reflect the influence of their aromatic and alkyl substitutions. As illustrated (Fig. 9), the conformation of the active analogs

*A feature of the Diels-Alder reaction involves the stereochemical orientation of the addends. These additions favor the orientation which has the diene double bonds close to the unsaturated substituents of the dienophile and is designated *endo* (inside). Thus, the substituent is directed to the convex side of the resulting cyclohexene ring. Conversely, *exo* (outside) has the substituent directed to the concave side of the ring.

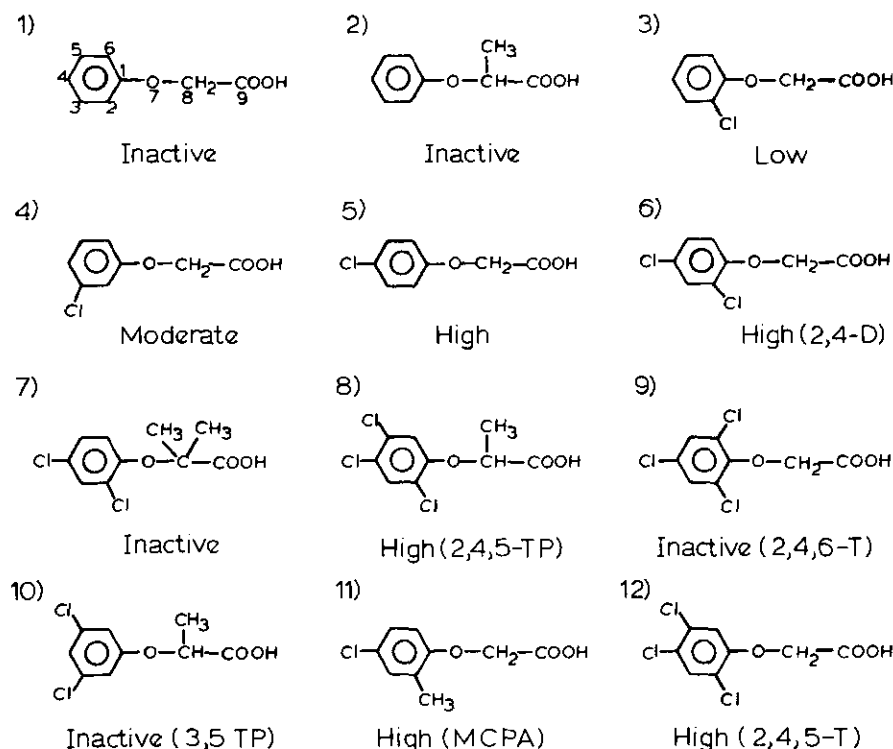


FIGURE 8. Phenylalkanoic acid herbicides.

can be planar (2,4,5-T) or, as in 2,4,5-TP, the carboxy function is perpendicular to the plane of the rest of the molecule. The inactive analog 2,4,6-T has the sidechain perpendicular to the phenyl ring. However, in the inactive 2-methyl analog, the acid function is nonplanar, as observed for 2,4,5-TP.

Conformational energy calculations have not been carried out, but free rotation about the ether-acetate bond is expected. Calculations of the charge-density distribution within these compounds could show differences that might indicate why symmetrically substituted phenyl ring compounds are inactive.

Polyhalogenated Aromatic Hydrocarbons. The halogenated aromatic hydrocarbons most prevalent in the environment are the polychlorinated (PCB) or brominated (PBB) biphenyls (Fig. 10) whose lipophilic properties lead to their accumulation in many tissues. However, one of the most toxic is 2,3,7,8-tetrachlorodibenzo-*p*-dioxin (dioxin), a trace by-product in the synthesis of 2,4,5-T (1,2). There are 75 possible chlorine substituted dioxin isomers and their toxicity depends upon both the number and position of the halogens. Since a number of these halogenated aromatic hydrocarbons are formed as trace contaminants in the synthesis of several commercial products, structure-activity relationships have been derived in order to understand their mechanisms of bioactivity (33-40).

A number of PCBs and dioxin analogs have been used as model compounds to investigate the specific structural requirements for cytosol receptor binding and for induction of aryl hydrocarbon hydroxylase activity (33-37). X-ray crystallographic analyses also have been carried out to elucidate their conformational properties (38-

42). As illustrated (Fig. 10), many of these compounds have common structural features.

Toxicological studies have further demonstrated that the most toxic PCBs and PBBs are those that have halogens in both the *meta* and *para* positions of both rings, but no *ortho* substituents (40). Crystallographic analysis of these biphenyls show that the most stable conformation is nonplanar, with the dihedral angle between the phenyl rings of 47° (39) (Fig. 11). Analysis of these compounds using molecular orbital techniques (43) shows that the minimum energy conformation of structures without *ortho* substituents is 42°, while it is 90° for *ortho*-substituted compounds, in agreement with the crystallographic results. However, activity data for the dioxin or naphthyl compounds indicate that a planar conformation is required for toxicity. Therefore, interpretation of these data suggests that the minimum requirements for toxicity include four halogens positioned laterally on the biphenyl rings, and a planar conformation.

However, more recent quantitative structure-activity data (37) indicate that molecular shape and polarizability are important factors in determining molecular reactivity and that hydrophobic, hydrogen bonding and electronic forces play a critical role in determining these properties. These data further suggest that halogen substitution in both phenyl rings is not a requirement for binding, nor is a planar structure. The molecular shape and thickness of these compounds will be affected by the conformation about the biphenyl bond and by the buttressing effects of adjacent halogens on the phenyl rings.

The results of these studies suggest that a model for

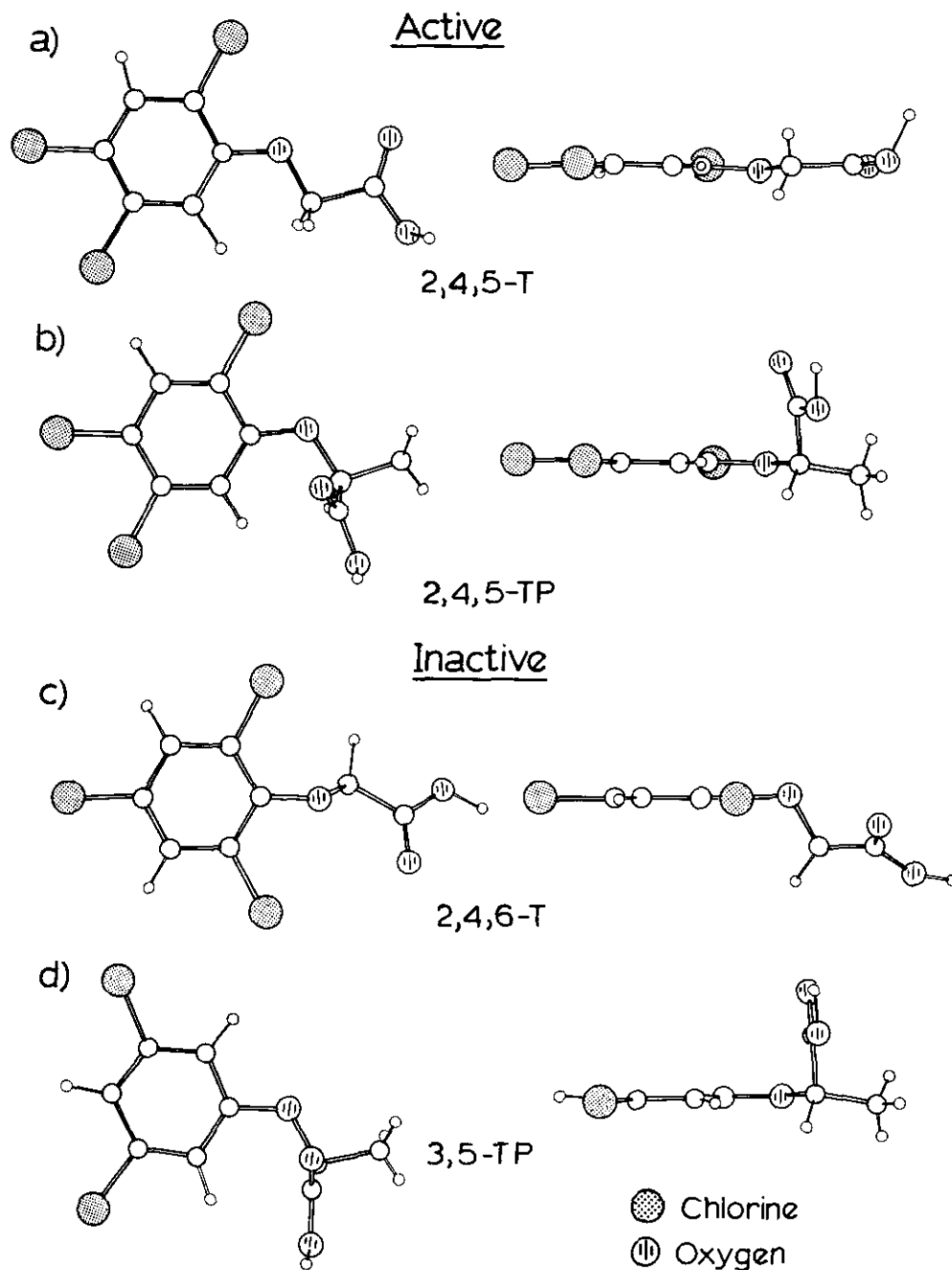


FIGURE 9. Crystal structures of phenylalkanoic acid insecticides (31,32), illustrating conformations observed for active and inactive analogs. Each molecule is viewed perpendicular to the phenyl ring and along its edge.

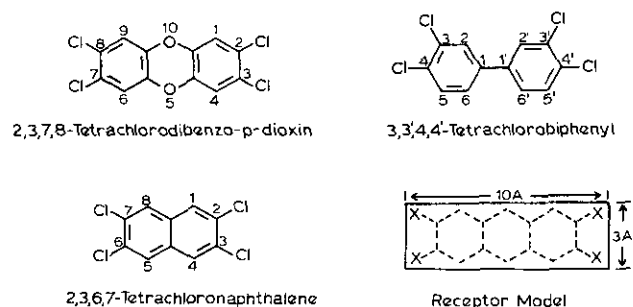


FIGURE 10. Examples of polyhalogen aryl hydrocarbon classes and a proposed receptor model (39) for active aryl hydrocarbons.

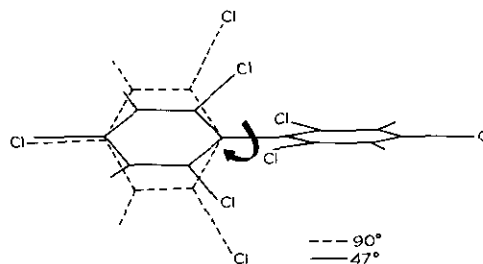


FIGURE 11. Conformational comparison of hexachlorobiphenyl (41) as observed in its crystal structure (dashed lines) with the rings perpendicular to each other, and with the rings rotated (47°), the proposed energy minimum model (solid lines) (39).

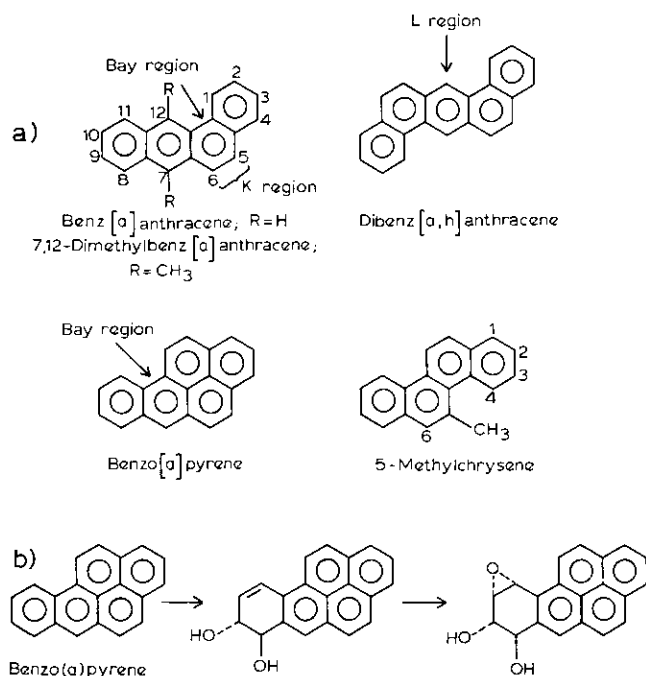


FIGURE 12. Carcinogenic polycyclic aromatic hydrocarbons (a) illustrating the reactive sites of the molecule and (b) showing the proposed steps in forming an epoxide diol structure.

toxic structures requires four lateral chlorines arranged in a box of approximate area $3 \times 10 \text{ \AA}$, or if brominated, three lateral bromines arranged in a triangle (40) (Fig. 10). This area defines the surface of the smallest envelope that a planar molecule may occupy and elicit its toxic response at its target site.

Polycyclic Aromatic Hydrocarbons. Many of the polycyclic aromatic hydrocarbons (PAH) that are carcinogenic are derived from a benzo[a]anthracene skeleton (Fig. 12). Structure-activity data show that the carcinogenic properties of this large class of PAHs are highly stereospecific and depend upon their chemical structure (1,44,45). It was also noted that most carcinogenic PAHs contain an angular three-ringed phenanthrene unit and that the greatest chemical reactivity is associated with the 5-6 bond, called the K region (Fig. 12). Thus, the earliest structure-activity profiles related the electronic structure of these compounds to their carcinogenicity (45). Recent data now suggest that their carcinogenic action is related to their metabolism involving arene oxides, dihydrodiols and diol epoxide formation (Fig. 12b).

Although a large number of polycyclic aromatic hydrocarbon metabolites have been identified, especially those of benzo[a]pyrene (BP), the ultimate carcinogen is believed to be an epoxide dihydrodiol formed by the action of mixed function oxygenase enzymes. These enzymes can produce two diastereoisomeric diol epoxides, designed by the disposition of the epoxide function with respect to the hydroxy group. Thus, the *syn* isomer has the epoxide and hydroxy on the same side of the ring, while the *anti* has them on opposite sides. These data

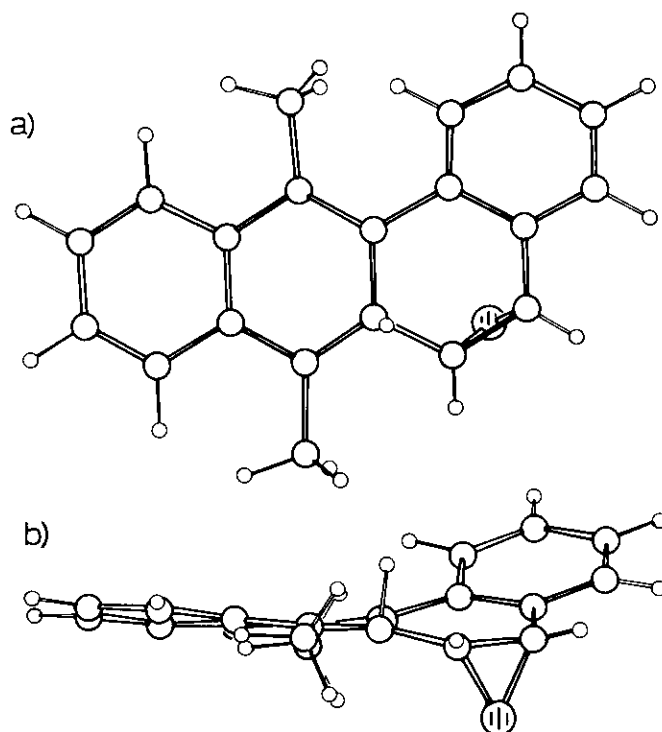


FIGURE 13. Crystal structure of 7,12-dimethyl-5,6-epoxy benzo[a]pyrene (52) viewed (a) perpendicular to the pyrene ring system and (b) parallel to the ring system, illustrating the bay region crowding and distortion of the rings.

show that the mutagenic and carcinogenic properties of these isomers differ greatly. The *anti* isomer has been identified as the ultimate carcinogen (45), while the *syn* isomer is more mutagenic. Additionally, K region oxides and diol epoxides have been shown to bind covalently to nucleic acids (44-47).

Crystallographic studies of many of the more potent carcinogenic PAHs have been carried out and show important conformational differences when compared with their non carcinogenic parent hydrocarbons (46,47). Many of the PAHs are planar, whereas their methylated derivatives are nonplanar due to the steric interactions of the methyl hydrogens with those of the polycyclic ring hydrogens, particularly in the crowded Bay region of the molecule (Fig. 13). This is the case for the most potent carcinogenic PAHs, 7,12-dimethylanthracene (DMBA) and 5-methylchrysene.

More recent structural data have investigated the stereochemistry of BP diol epoxides using naphthalene derivatives as model compounds (48-52). These data reveal that in the structure of the 2-methyl BP analog, 3,4-epoxy-2-methyl-1,2,3,4-tetrahydro-1-naphthol, the hydroxy and epoxide oxygens are *syn* and there is an internal hydrogen bond between them that persists in solution (48). In the structure of the *anti* 3,4-dihydroxy-1,2,3,4-tetrahydronaphthalene-1,2-oxide isomer (51), the two hydroxy groups are equatorial, as observed in the BP epoxide (52). The epoxide oxygen does not participate in any hydrogen bonding as observed in the *syn* 2-methyl analog (48).

The stabilities of these epoxy diol BP analogs have been computed using quantum mechanical methods (53) which show that the *cis* axial-axial diol epoxide is the more reactive species; however, no intramolecular hydrogen bond was indicated. More recent data using molecular shape analysis of polycyclic aromatic hydrocarbons indicate that the quantitative structure-

activity relationships derived can be used to estimate the mutagenic potency without explicit consideration of metabolic activation pathways (54).

Thus, these studies have led to definitive information concerning specific structural parameters of importance for the mutagenic and carcinogenic characteristics of these compounds. While these data have helped shape the concepts of carcinogenicity, there still remains much to be learned about how these stereospecific interactions signal their molecular reactivity.

Pharmacological Agents

In contrast to the toxic properties associated with environmental agents, pharmacological or therapeutic agents are biologically active compounds which, when applied appropriately, modify physiological systems for the benefit of the recipient. Since many pharmacologically important drugs act by inhibiting enzymes, kinetic studies of their inhibitory effects provide valuable information on their potency and mechanisms of action. Therefore, studies of drug (or hormone) action are concerned with understanding the relationships observed between drug structure and biological activity, and developing a receptor theory to account for these observations.

The receptor can be characterized by describing the properties of compounds that react with it, thus producing a "negative replica" of the receptor from the composite of the structure-activity information assembled. Compounds that combine with the receptor and produce a change in cellular properties are agonists, while those that combine with it, but do not elicit the given responses are antagonists. Understanding these

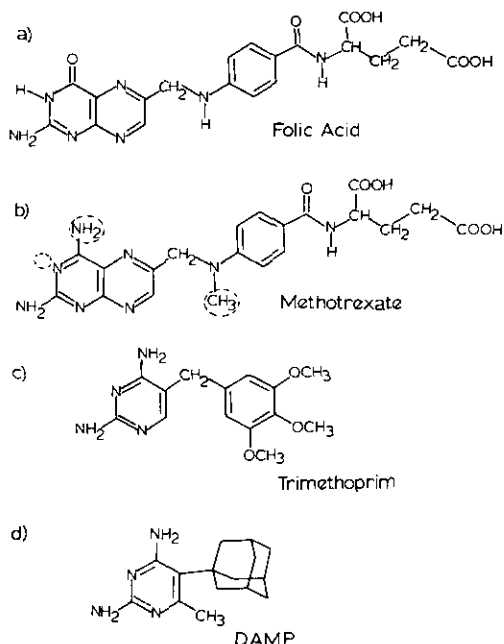


FIGURE 14. Substrates and inhibitors of dihydrofolate reductase: (a) folic acid, natural substrate; (b) methotrexate, species-nonspecific reductase inhibitor; (c) trimethoprim, bacterial reductase inhibitor; (d) DAMP, mammalian reductase inhibitor.

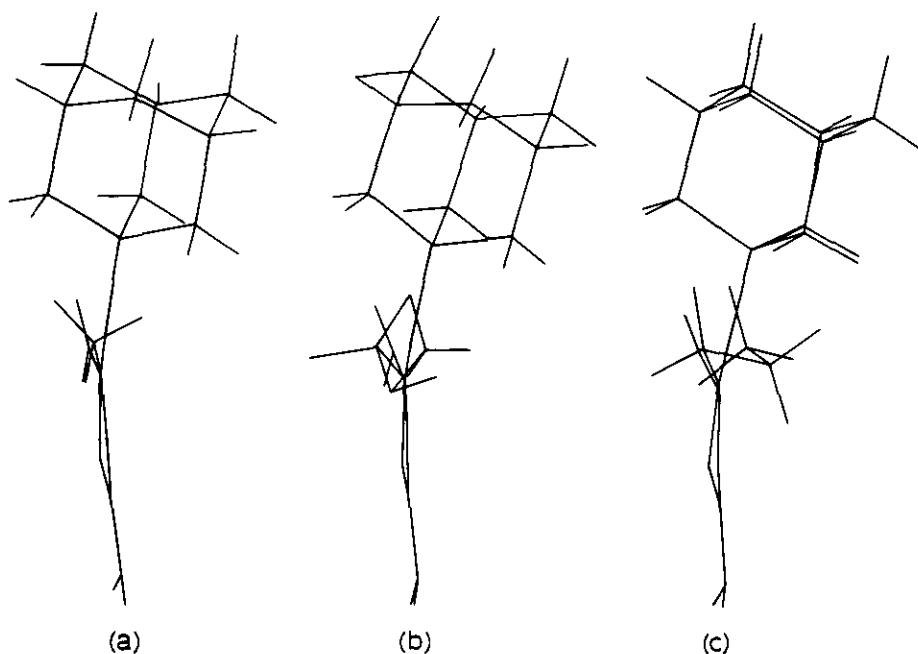


FIGURE 15. Profile view of the antineoplastic DHFR inhibitors showing the "bowing" caused by the pyrimidine ring distortions (58): (a) DAMP (55); (b) DAEP; (c) DAPP.

data are not straight forward since there are many types of competition that can arise with the interaction of a drug with its receptor site.

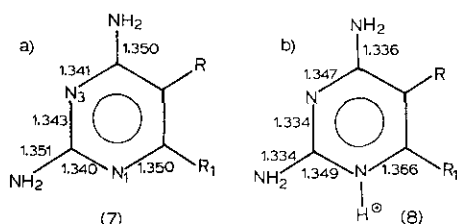


FIGURE 16. Comparison of the average diaminopyrimidine nitrogen geometry observed from their crystal structures (56) for (a) unprotonated and (b) N1 protonated structures. The figures in parentheses refer to the number of structures included in the averages.

Although there are several examples of pharmacologically important agents that have been studied crystallographically, only dihydrofolate reductase inhibitors and thyroid hormone analogs will be examined in detail. Steroid hormone structures are described in another paper in this issue.

Dihydrofolate Reductase Inhibitors. The enzyme dihydrofolate reductase (DHFR), a necessary component for all cell growth, is strongly and specifically inhibited by certain substrate analogs with binding affinities so great that they are not readily displaced by the natural folic acid substrates (Fig. 14). It has been shown that the general requirement for tight binding of inhibitors to DHFR from any species is a 2,4-diaminopyrimidine ring structure (55). Also, the binding

IODOTHYRONINE DEIODINATION

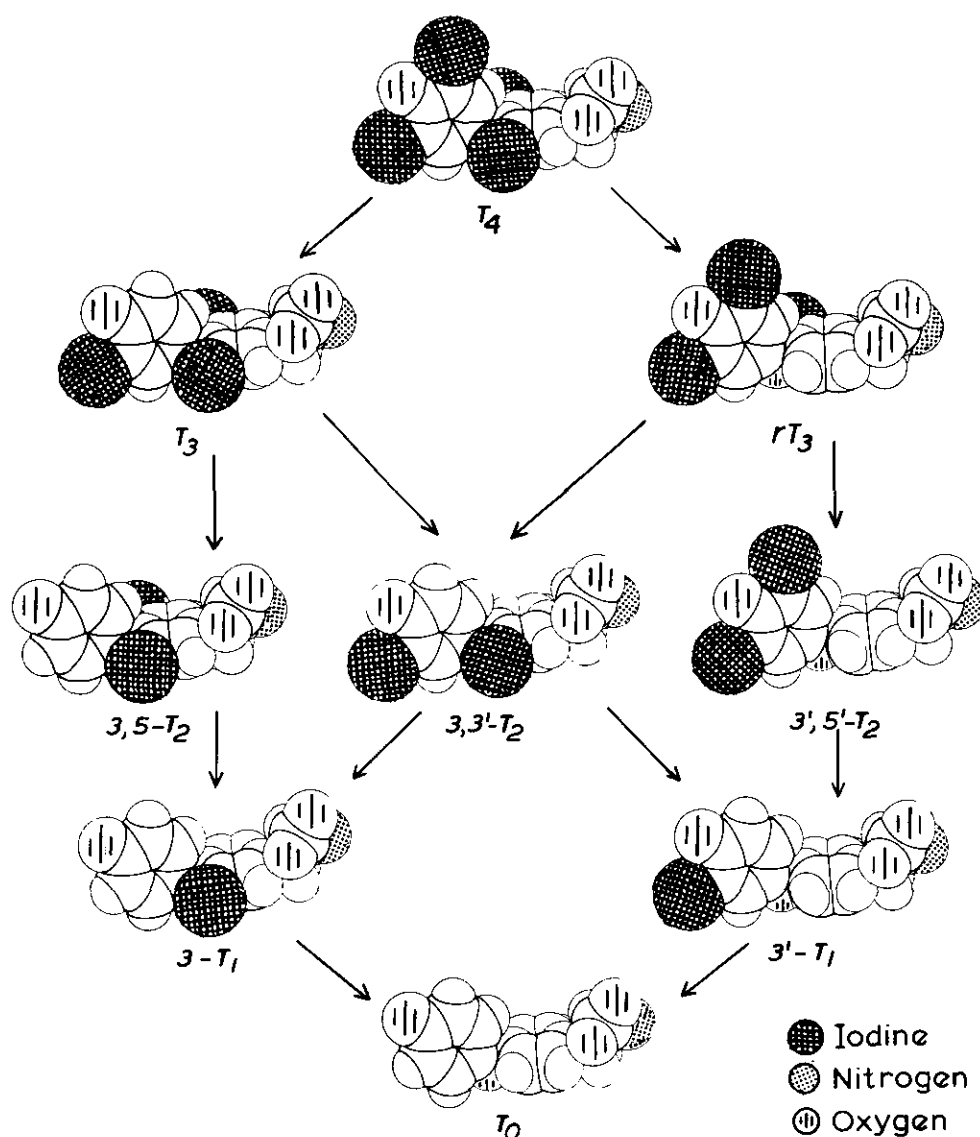


FIGURE 17. Iodothyronine deiodination pathway of the thyroid hormone thyroxine (T_4) to the hormonally active (T_3) metabolites and hormonally inactive (rT_3) metabolites.

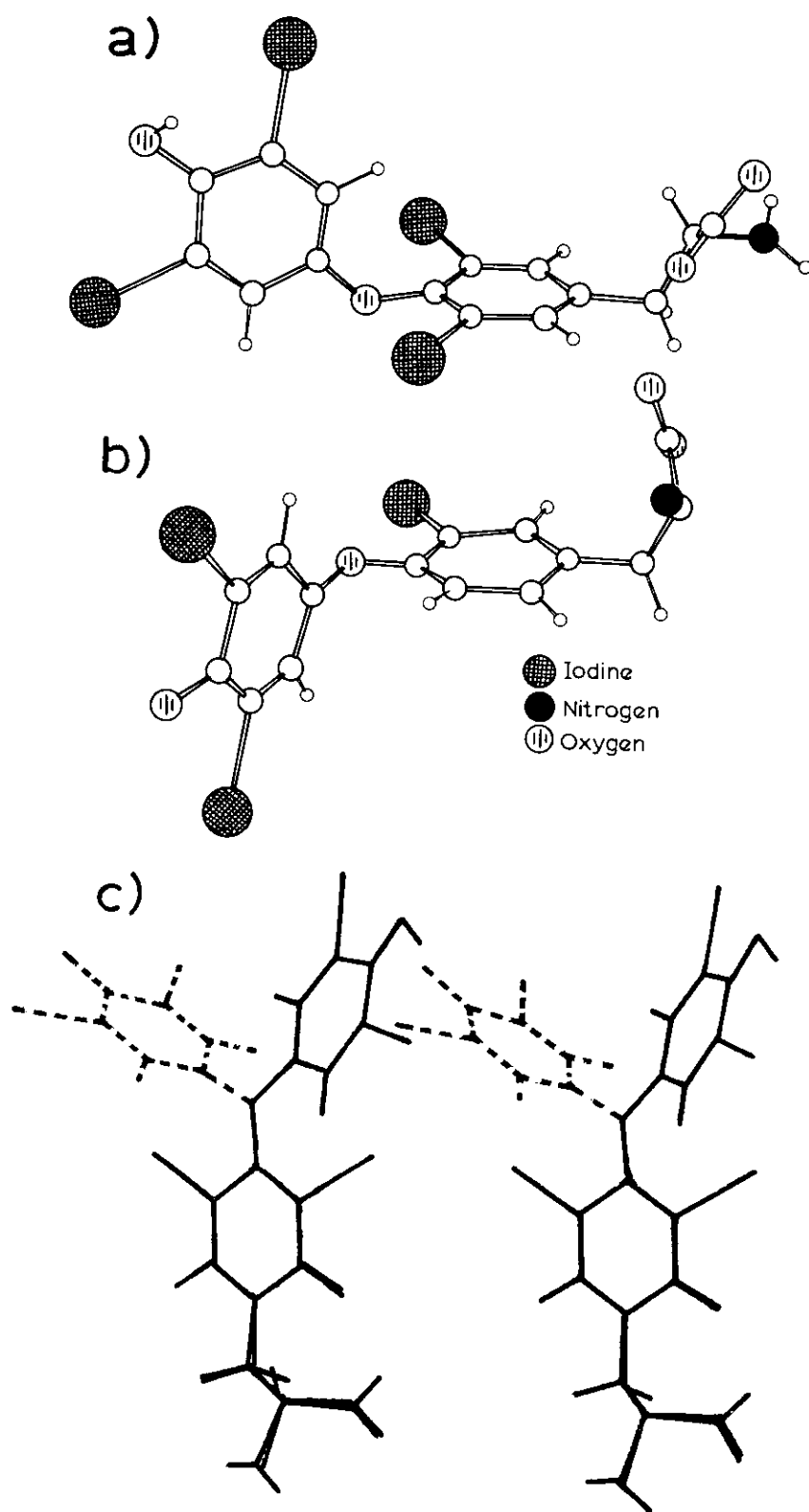


FIGURE 18. Molecular structures of thyroid hormones with a (a) skewed diphenyl conformation (T₄) (66) and (b) antiskewed rT₃ (67); (c) the stereo overlap of the skewed (...) and antiskewed conformations.

selectivity and specificity of inhibitors for DHFR from different species can vary significantly with only a single substituent change.

Comparison of several lipophilic 5-substituted analogs show that those with a 5-adamantyl substituent are the most effective inhibitors of mammalian DHFR and possess significant antineoplastic activity (56). For example, there is a 500-fold increase in inhibitory potency within this series of 5-adamantyl-6-substituted antifolates with 6-H < propyl < methyl < ethyl. In order to investigate the conformational aspects of binding specificity to DHFR, crystallographic analyses were carried out on this series and their results compared with the structural data from other antifolate classes (57-63). These data reveal that the most striking feature of these adamantyl antifolates is their "bowed" shape (Fig. 15), caused by the steric crowding of the 5-adamantyl and the 4- and 6-substituents. This interference forces the pyrimidine ring to be significantly distorted from planarity. These data further demonstrate the effects of N1 protonation of the pyrimidine ring geometry. Comparison of the endocyclic bonds at C2 (Fig. 16) indicates that protonation causes the N1-C2 bond to lengthen and the C2-N3 bond to decrease (58). To investigate the significance of these structural changes to the binding energies and basicity of these compounds, CNDO/2 molecular orbital calculations were carried out (64) and were able to reproduce the pyrimidine ring torsional distortions observed in their crystal structures, as well as the geometry changes upon protonation at N1. The rotational energy barrier was also computed and showed that the minimum energy conformation was the same as observed in the crystal structure. However, these calculations were not able to accurately reproduce the exocyclic amino geometry and this discrepancy can affect the charge density distributions within the pyrimidine ring.

Pyrimidine antifolates with a 5-benzyl substituent, such as trimethoprim (TMP) (Fig. 14), have the greatest selectivity in their binding for bacterial DHFR. Structural studies of TMP (59,60) show that it can adopt several equi-energy conformations. Structure-activity data show that those TMP compounds with a functionalized 4'-substituent are more potent than TMP itself. Analysis of the 4'-isopropenyl and 4'-carbomethoxy derivatives (59) shows that these substituents are perpendicular to the benzyl plane and, unlike TMP, place density both above and below the ring plane.

Structural studies have also been carried out on the natural substrate folic acid (63) and show that the overall molecular shape is similar to that of the inhibitor methotrexate as observed in the protein structures of DHFR from bacterial sources (65). Quantum mechanical and dynamic energy calculations have also been carried out on the folate molecules (66,67), and these results show that there is considerable flexibility in the orientation of the side chains and that the low energy conformation corresponds to that found in the crystal structures.

As a result of these studies the geometries of these

compounds have been accurately defined, as have their hydrogen bonding patterns and conformational and electronic properties. These observations may explain their antifolate characteristics and provide a means for the rational design of more selective antifolates.

Thyroid Hormone Structures. Thyroid hormones (Fig. 17) are secreted from the thyroid gland into the general circulation where they are bound to one of several serum proteins. These hormones are also the only halogenated molecules that are biologically active, and have a number of specific proteins and enzymes that transport and metabolize them. Therefore, it is of interest to speculate on the role that these thyroid proteins and enzymes may have in the concentration and transport of other halogenated species. As observed, many of the most toxic environmental agents are halogen-containing compounds. Therefore, the possibility exists that these compounds could be recognized by these thyroid hormone specific proteins.

Structural studies carried out on the thyroid hormones and their analogs (68) have shown that these molecules are flexible and that each of the hormone-specific binding proteins requires a different conformation for maximal binding affinity. The specific stereochemical properties of the thyroid hormones arise from the steric influence of the *diortho* inner ring iodines upon the diphenyl ether conformation. Minimal steric interaction between the 3,5-iodines and the outer ring 2',6'-hydrogens is maintained when the conformation is skewed (e.g., the two rings are mutually perpendicular and bisecting). Because of the restricted rotation about the ether bridge, the crystal structures of all *diortho*-substituted thyroactive analogs have a skewed conformation (68), while that of 3',5',3-triiodothyronine, (rT₃) (69) is antiskewed (Fig. 18).

Conformational analysis of the crystallographic data permits the delineation of characteristic patterns within these structures that can be correlated with their hormone action. These data show that there exist preferred orientations of hydrogen bonds and iodine intermolecular contacts that can indicate spatial preferences for critical functional groups within the binding environment of a hormone responsive protein or enzyme (9,70).

Of particular interest in the mechanism by which the thyroid hormones are deiodinated (Fig. 17). The most active form of the hormone, 3,5,3'-triiodothyronine (T₃), is derived from the deiodination of thyroxine (T₄) in peripheral tissues. The enzyme iodothyronine deiodinase produces either metabolically active (T₃) or inactive (rT₃) products (Fig. 17). Structure activity studies of the inhibition of this enzyme (70-72) by a variety of compounds including radiographic contrast agents, dyes, and flavones indicate that the enzymes recognition process is under stereospecific control involving stringent requirements for maximal inhibition. Many of these inhibitors are of concern since their ingestion can interrupt normal thyroid function and lead to physiological problems. Such is the case with the radiographic contrast agents which have slow rates of metabolic clearance and have been shown to cause hypothyroidism by

FLAVONOID CLASSIFICATIONS

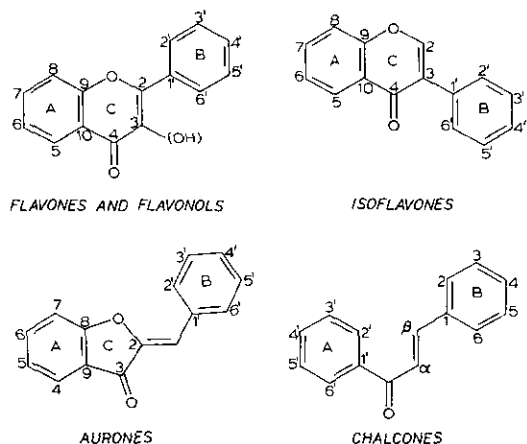


FIGURE 19. Flavone classes.

inhibition of the deiodination pathway (73).

Flavones are ubiquitous natural products (Fig. 19) derived from plant pigments. Aurones are the most potent inhibitors of iodothyronine deiodinase (74). In an effort to identify structural features common to natural substrates and inhibitors of the deiodinase enzyme, three conformational models of the most potent aurone, aureusidin, were compared with the observed crystal structures of the thyroid hormones (Fig. 20) (75). The skewed conformation is not a permitted aureusidin conformation since it requires rotation about the bridging double bond. This, on the other hand, is the conformation observed for all hormonally active thyroid compounds (68). A planar structure is also an energetically favorable aurone conformation, but not one that can be adopted by the thyroid compounds. Finally, the anti skewed conformation has been observed in the crystal structure of rT_3 , a natural inhibitor of deiodinase, and is a likely aurone conformation. Thus, these studies suggest that the deiodinase enzyme can bind a substrate or inhibitor in either the skewed or antiskewed conformation.

Receptor Models

Since crystal structures of the protein-substrate complex have been determined for dihydrofolate reductase and prealbumin, many previously proposed hypotheses concerning the structural basis for binding and activity of the antifolate and thyroid hormones can be tested. The results of the crystal structure determination of DHFR from four species, complexed with the cofactor NADPH and with inhibitors (65,76), provide specific information concerning the backbone conformation, spatial arrangement of the side chains, and a general description of the inhibitor binding site.

Computer graphic modeling of the fit of various inhibitors in the active site of DHFRs has been undertaken. Lipophilic antifolate binding to chicken liver

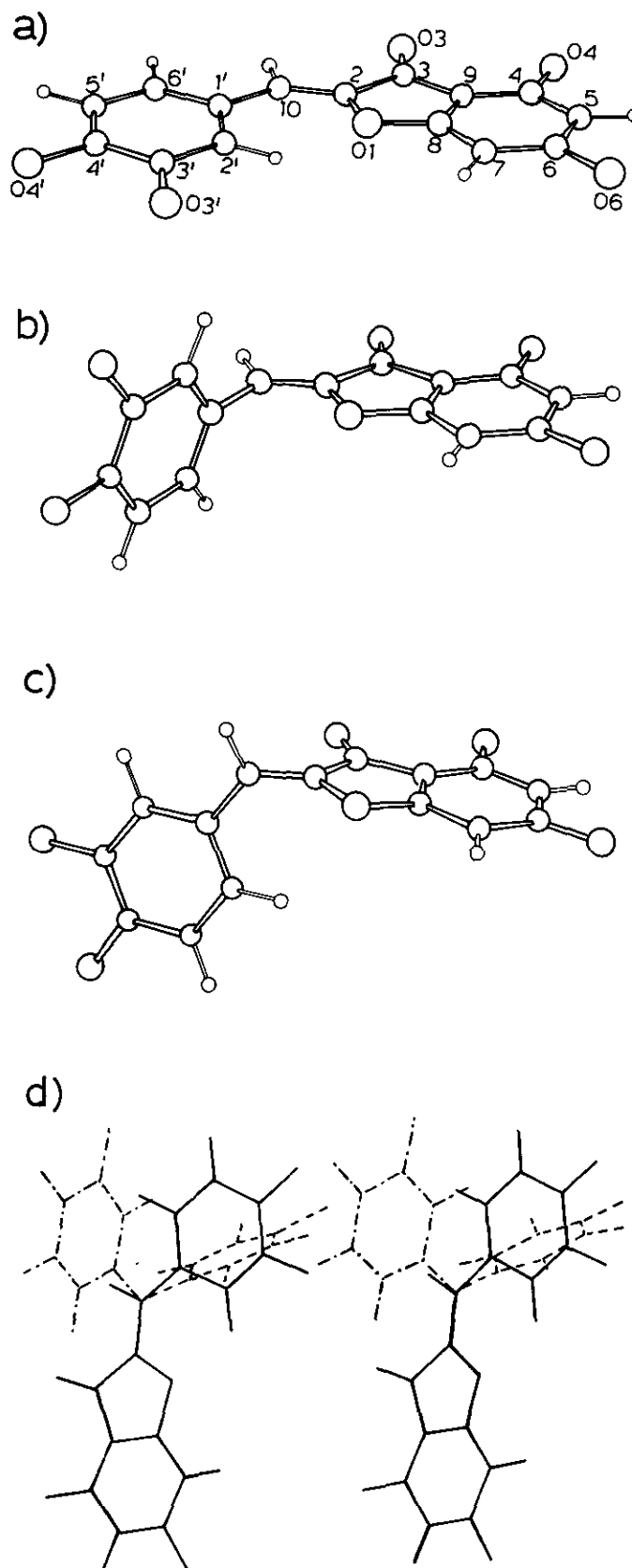


FIGURE 20. Aureusidin conformational models: (a) planar; (b) anti-skewed; (c) skewed; and (d) stereo overlap of all three.

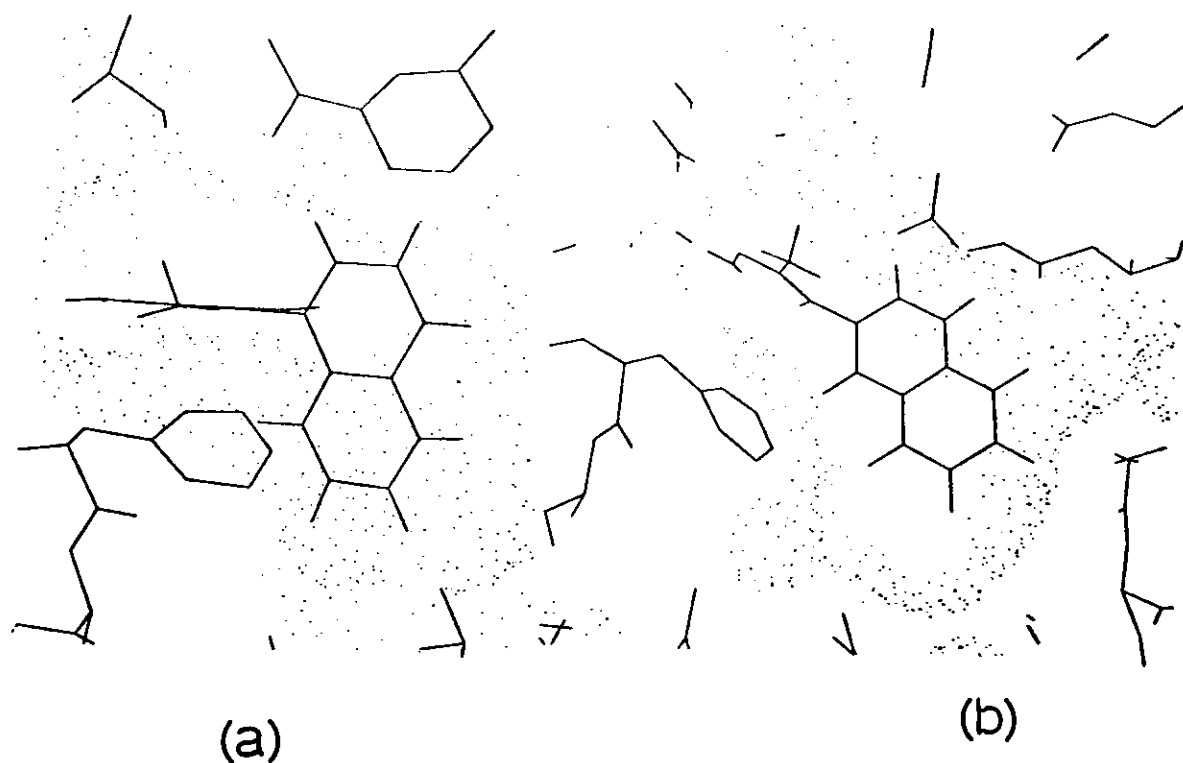


FIGURE 21. Binding models of (a) 1-naphthyldiaminopyrimidine (55) in the active site of chicken liver DHFR (76), showing the poor fit of the naphthyl ring in the binding pocket; (b) 2-naphthyldiaminopyrimidine in the same site which shows no steric interference. The stippling is the protein surface.

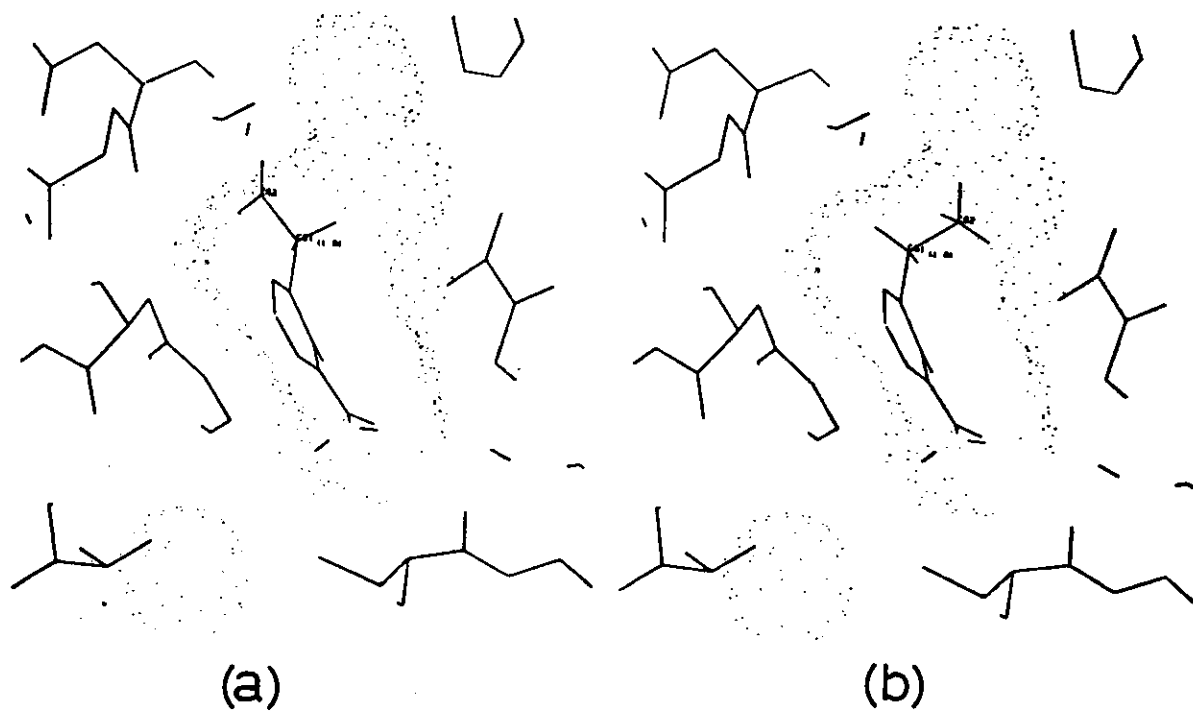


FIGURE 22. Binding models of (a) DAEP in the active site of chicken liver DHFR; (b) with the ethyl side chain rotated 110° and fit into an alternate binding pocket.

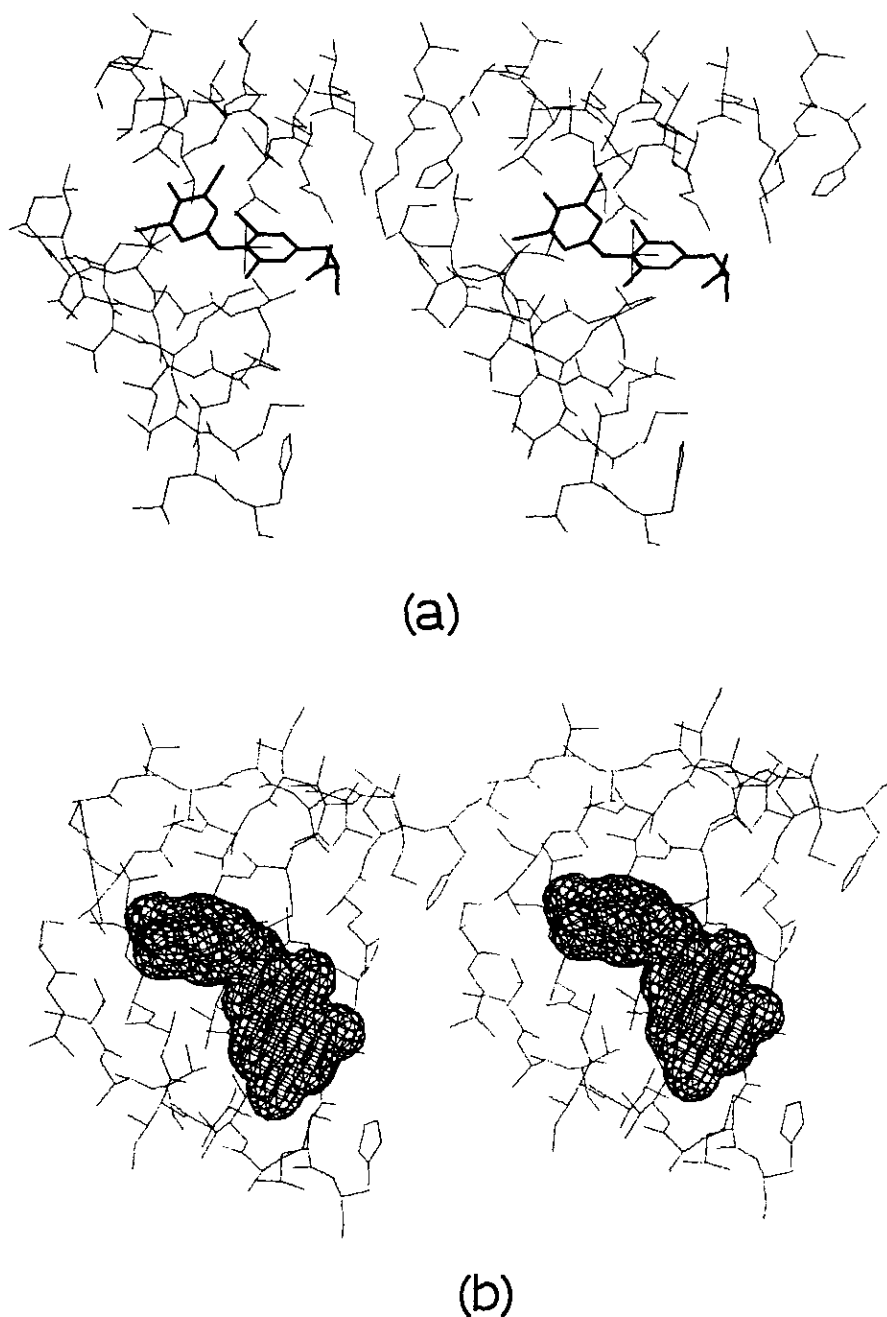
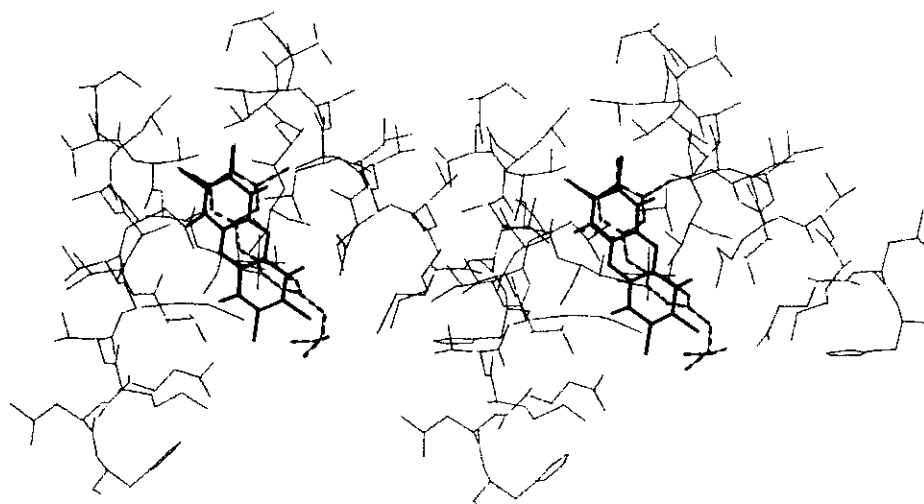


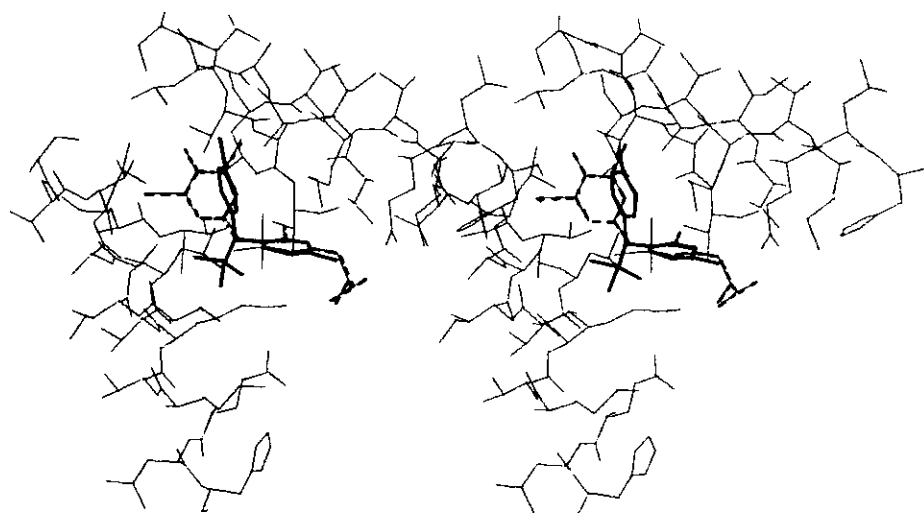
FIGURE 23. Stereo diagrams of (a) the thyroxine binding site in the crystal structure of prealbumin (77); (b) of the binding of aureucidin in an antiskewed conformation with its phenyl ring matched to the outer ring of thyroxine of prealbumin. (The van der Waals surface of aureucidin is also shown);

DHFR was modeled by positioning the diaminopyrimidine ring in the same orientation as observed structurally for the diaminopteridine ring of methotrexate (57). This orientation was also verified from crystallographic studies of the binary complex of chicken liver DHFR and DAMP (Matthews, personal communication). These observations showed that there is no steric crowding of the adamantyl ring in the binding cavity. However, when the structure of the 5-(1-naphthyl)diaminopyrimidine, a noncompetitive inhibitor (57), was modeled in the same manner, the outer portion of

the naphthyl ring penetrates through the surface of the binding pocket and comes into close contact ($< 1.3 \text{ \AA}$) with a phenylalanine residue (Fig. 21a). Even when the naphthyl ring is rotated, there is no satisfactory orientation for the ring. On the other hand, when the active 2-naphthyl analog is similarly modeled, there are no unfavorable interactions (Fig. 21b). More subtle features of the inhibitor-substrate interactions are observed when the binding of the 6-ethyl adamantyl structure is compared with that of the less active 6-methyl analog. Figure 22a focuses on the 6-ethyl posi-



(c)



(d)

FIGURE 23. (c) The binding of dioxin (42) with its chlorophenyl ring matched to the outer phenyl ring of thyroxine in the prealbumin binding site (The van der Waals surface of dioxin is also shown.); (d) DDT (14) with its *p*-chlorophenyl ring matched to the inner ring of thyroxine in the prealbumin binding site.

tion of the antifolate structure as observed from its crystal structure (58), while Figure 22*b* shows that a 110° rotation of the ethyl sidechain places the outer carbon in an alternate binding pocket that appears to be more suitable. This observation would suggest that the ethyl analog is more active because of the added hydrophobic interactions with the enzyme and that there is not sufficient room to fit the propyl sidechain in this pocket, hence its lesser activity.

Similar observations have been made for the binding interactions of the thyroid hormones with the serum protein prealbumin (77). Prealbumin is composed of four

identical subunits that form a channel running through the length of its structure, forming the thyroxine binding site. These structural data also provide a detailed environment for the iodine atoms of the hormone as well as a quantitative description of the iodine interactions in the active site (Fig. 23*a*). Iodothyronine analogs that are potent inhibitors of iodothyronine deiodinase are also strong binders to thyroxine-binding prealbumin. Because of this similarity, the thyroxine binding site in the crystal structure of prealbumin was used as a model for the active site of iodothyronine deiodinase. As illustrated (Figs. 23*b* and *c*) both the planar and anti-

skewed models for aureucidin are able to fit into the thyroxine binding site of prealbumin, suggesting a mode of inhibitor recognition. This model helps explain the iodothyronine analog inhibition data and suggests that more specific enzyme inhibitors can be designed.

Since the halogenated pollutants such as dioxin, DDT or the phenylalkanoic acid insecticides may bind to the thyroid hormone specific proteins in much the same manner as the thyroid hormones, models of their binding to the active site in prealbumin were also studied. As shown (Fig. 23), these compounds can fit into the thyroxine binding site and position at least one of their chlorines in an iodine binding pocket. These toxic agents can be accommodated in the binding site with their ring structures matched to either the inner or outer phenyl ring of thyroxine. While these models show that these pollutants can fit into the binding channel of prealbumin, the data for the deiodinase inhibitors suggest that not all of the inhibitor structure need overlap the thyroid hormone to elicit enzyme recognition. Therefore, these studies indicate the type of possible interactions that may be operative in the concentration of these pollutants by the thyroid hormone proteins.*

Summary

This paper has described the role of X-ray crystallographic data in delineating those structural characteristics that are relevant for enhanced active-site binding and function among a series of environmental and pharmacological agents. These examples show how structural data were used to define absolute configuration, molecular shape, conformational flexibility and active-site topology.

For example, structural analysis of the synthetic pyrethroid insecticides has defined the absolute stereochemistry of the three chiral centers in the molecule and demonstrate the importance of conformation to the stereoselectivity of these compounds. The presence of a *cis* or *trans* configuration of the functional groups attached to the cyclopropane ring has a dramatic influence on the overall shape of the molecule with the (S)*cis*(1R,3R) configuration being required for maximal activity.

Within the series of DDT analogs, analysis of the diphenyl ring conformation indicates that there is a narrow range of values permitted for the most toxic compounds. These data further show that the overall shape of the molecule is important and that there is a steric size and aromatic character prerequisite for the bridging groups to elicit maximal toxicity.

Structural analysis of the phenylalkanoic acid herbicides indicates that factors other than molecular conformation dominate the structure-activity relationships since the active and inactive analogs can have the same conformation. These data, however, do suggest that the

charge-density properties of these compounds are of importance to activity. Thus, the availability of accurate geometrical parameters for this series of compounds is a necessary starting point for these calculations.

Similarly, structural analysis of the lipophilic antifolates has shown that adamantyl substitution causes distortion of the pyrimidine ring planarity by steric crowding with adjacent ring substituents. This results in an overall "bowed" shape to the molecule and could explain the enhanced antineoplastic activity of this family of compounds compared with other antifolates with similar lipophilicities. Furthermore, the crystal structure determination of DHFR from several species has permitted observation of the active site and modeling of the binding of other antifolates within it. These studies have defined the conformational space available for binding and have delineated the important interactions of the inhibitor-enzyme binding complex and have further permitted the rational design of other inhibitors.

Perhaps most importantly, this type of structural study now permits a more realistic interpretation of structure-activity relationships of systems where no specific structural data are yet available. For example, use of structural data from a related family of proteins to model the inhibitor-enzyme complex permits a more precise description of the types of interactions that are important. This approach is demonstrated in the interpretation of the structure-activity relationships among flavones as potent inhibitors of the enzyme iodothyronine deiodinase. By using the thyroxine binding site of prealbumin as a model, correlations were observed that could help explain the mode of action of these compounds. In a similar manner, this site was also used to explore the possible binding modes accessible to the halogenated environmental agents such as dioxin and DDT and in this way show a mode of entry of these species into tissues.

The future will see a greater emphasis on the input of specific and well-determined structural data, and as more protein structures and enzymes become available from solid state and solution, the "negative replica" of the receptor will develop into a clear "picture" of the active site mechanism of action of these important systems.

The author thanks Catherine DeVine, Danielle Smith and Yi-Yan Hong for their efforts in preparing the data for computer analysis and for the literature searches; Melda Tugac, Gloria DelBel, and Queen Bright for graphic illustrations, and Dr. William Duax for his critical review of this manuscript. Molecular volumes were computed by using a pseudoelectron density function computed on the MMS-X graphics display system, designed and fabricated by the Computer Systems Laboratory, Washington University, St. Louis. This research was supported in part by a grant from AM-15051.

*Recent workers have provided experimental evidence for their modeling predictions that chlorinated dibenzodioxins and dibenzofurans can be effective competitive binding ligands for thyroxine binding sites in prealbumin (78).

REFERENCES

1. Doull, J., Klaaseen, C. D., and Amdur, M. O. Cassarett & Doull's Toxicology: The Basic Science of Poisons. Macmillan Publishing Co., New York, 1980.
2. Nicholson, W. J., and Moore, J. A., Eds. Health Effects of Halogenated Aromatic Hydrocarbons. New York Academy of Sciences, New York, 1979.
3. Elliott, M., and Janes, N. F. Synthetic pyrethroids—a new class of insecticide. *Chem. Soc. Rev.* 1978: 473-505.
4. Begley, M. J., Crombie, L., Simmonds, D. J., and Whiting, D. A. X-ray analysis of synthetic (4S)-2-(prop-2-enyl)rethron-4-yl (1R,3R)-chrysanthemate 6-bromo-2,4-dinitrophenylhydrazide and chiroptical correlation with the six natural pyrethrin esters. *J. Chem. Soc. Perkin I*, 1974: 1230-1235.
5. Owen, J. D. Absolute configuration of the most potent isomer of the pyrethroid insecticide α -cyano-3-phenoxybenzyl-*cis*-3-(2,2-dibromovinyl)-2,2-dimethylcyclopropanecarboxylate by crystal structure analysis. *J. Chem. Soc. Perkin I*, 1975: 1865-1868.
6. Owen, J. D. X-ray crystal structure of two pyrethroid insecticides: *cis*-3-phenoxybenzyl-3-(2,2-dibromovinyl)-2,2-dimethylcyclopropanecarboxylate and the 3-(2,2-dichlorovinyl) analog. *J. Chem. Soc. Perkin I*, 1976: 1231-1235.
7. Owens, J. D. Structure of *rel*(α R), (1R,*trans*)- α -cyano-3-phenoxybenzyl-3-(2,2-dichlorovinyl)-2,2-dimethylcyclopropanecarboxylate. Non insecticidal components of cypermethrin. *Acta Cryst.* B37: 1131-1134 (1981).
8. van der Heijden, S. P. N., Griffith, E. A. H., Chandler, W. D., and Robertson, B. E. Conformations of bridged diphenyls. VII. Crystal structure of 2-(4'-carbomethoxy-2'-nitrophenoxy)-1,2,3-trimethylbenzene. *Can. J. Chem.* 53: 2084-2092 (1975).
9. Cody, V. Thyroid hormone-receptor interactions: binding models from molecular conformation and binding affinity data. In: *Computer-Assisted Drug Design* (E. C. Olson and R. E. Christofferson, Eds.), ACS Symposium Series No. 112, American Chemical Society, Washington DC, 1979, pp. 281-299.
10. Janes, N. F. The pyrethrins and related compounds. Part 21. Carbon-13 nuclear magnetic resonance spectra of synthetic pyrethroids. *J. Chem. Soc. Perkin I*, 1977: 1878-1881.
11. Holan, G. New halocyclopropane insecticides and the mode of action of DDT. *Nature* 221: 1025-1029 (1969).
12. Mullins, L. J. The use of models of the cell membrane in determining the mechanism of drug action. In: *A Guide to Molecular Pharmacology-Toxicology*, Part I (R. M. Featherstone, Ed.), Marcel Dekker, New York, 1973, pp. 1-52.
13. DeLacy, T. P., and Kennard, C. H. L. Insecticides. Part I. Crystal structure of 1,1-bis-(*p*-chlorophenyl)-2,2-dichloropropane and 1,1-bis-(*p*-ethoxyphenyl)-2,2-dimethylpropane. *J. Chem. Soc. Perkin I*, 1972: 2141-2147.
14. DeLacy, T. P., and Kennard, C. H. L. Insecticides. Part II. Crystal structures of 1,1-bis-(*p*-chlorophenyl)-2,2,2-trichloroethane (*p,p'*-DDT) and 1-(*o*-chlorophenyl)-1-(*p*-chlorophenyl)-2,2,2-trichloroethane (*o,p'*-DDT). *J. Chem. Soc. Perkin II*, 1972: 2148-2153.
15. Smith, R. A., and Bennett, M. J. Insecticides. I. the crystal structure and absolute configuration of (-)-1-(*o*-chlorophenyl)-1-(*p*-chlorophenyl)-2,2,2-trichloroethane, (-)-*o,p'*-DDT. *Acta Cryst.* B33: 1126-1128 (1977).
16. Hovmoller, S., Norrestam, R., and Palm, T. B. Structural studies of polychlorinated hydrocarbons. IV. 2,2-Bis(*p*-chlorophenyl)acetic acid. *Acta Cryst.* B33: 377-381 (1977).
17. Shields, K. G., Kennard, C. H. L., and Robinson, W. Insecticides. Part 7. Crystal structures of 1,1-dichloro-2,2-bis-(*p*-chlorophenyl)ethylene (DDE) and 1,1-dichloro-2,2-bis(*p*-chlorophenyl)ethane (DDD). *J. Chem. Soc. Perkin II*, 1977: 460-463.
18. Shields, K. G., and Kennard, C. H. L. Insecticides. Part 8. Crystal structures of 1,1-bis-(*p*-chlorophenyl)acetic acid (DDA) and 4,4'-dichlorobenzophenone (DBP). *J. Chem. Soc. Perkin II*, 1977: 463-465.
19. Smith, G., Kennard, C. H. L., and Whitnall, J. 1,1-Dichloro-2,2-bis-(*p*-fluorophenyl)ethane (DFDD) $C_{14}H_{10}Cl_2F_2$. *Cryst. Struct. Comm.* 6:131-136 (1977).
20. Smith, G., Kennard, C. H. L., and Palm, T. B. 1,1-Bis-(*p*-methoxyphenyl)-2,2-dimethylpropane. *Acta Cryst.* B36: 1693-1695 (1980).
21. Hovmoller, S., Smith, G., and Kennard, C. H. L. 1,1-Dichloro-2,2-bis-(*p*-ethylphenyl)ethane (perthane), $C_{18}H_{20}Cl_2$. *Cryst. Struct. Comm.* 7: 589-593 (1978).
22. Soloway, S. B. Correlation between biological activity and molecular structure of the cyclodiene insecticides. *Adv. Pest. Control Res.* 6: 85-126 (1965).
23. DeLacy, T. P., and Kennard, C. H. L. Insecticides. Part III. Crystal structures of endrin (1,2,3,4,10,10-hexachloro-6,7-epoxy-1,4,4a,5,6,7,8,8a-octahydro-*endo*-1,4-*endo*-5,8-dimethanonaphthalene) and aldrin (1,2,3,4,10,10-hexachloro-1,4,4a,8,8a-hexahydro-*endo*-1,4-*exo*-5,8-dimethanonaphthalene). *J. Chem. Soc. Perkin II*, 1972: 2153-2158.
24. Kennard, C. H. L., Smith, G., and Hovmoller, S. 1,2,3,4,10,10-Hexachloro-1,4,4a,5,8,8a-hexahydro-*endo*-1,4-*endo*-5,8-dimethanonaphthalene (isodrin). *Acta Cryst.* B35: 493-495 (1979).
25. Gress, M. E., and Jacobson, R. A. 1,2,3,4,10,10-Hexachloro-6,7-*exo*-epoxy-1,4,4a,5,6,7,8,8a-octahydro-*endo*-*exo*-1,4,5,6-dimethanonaphthalene (dieldrin), $C_{12}H_8Cl_6O$. *Cryst. Struct. Comm.* 3: 485-489 (1973).
26. Kennard, C. H. L., Smith, G., and White, A. H. Dihydrophotoaldrin acetate, $C_{14}H_{12}Cl_6O_2$. *Acta Cryst.* C39: 1701-1703 (1983).
27. Shields, K. G., and Kennard, C. H. L. Insecticides. Part IV. Crystal structure of heptachlor (racemic 1,4,5,6,7,8,8a-heptachloro-3a,4,7,7a-tetrahydro-4,7-methanoindene). *J. Chem. Soc. Perkin II*, 1973: 1374-1376.
28. Hovmoller, S., Smith, G., and Kennard, C. H. L. Racemic 1-*exo*-4,5,6,7,8,8a-heptachloro-*exo*-2,3-epoxy-3a,4,7,7a-tetrahydro-4,7-methanoindene (heptachlor epoxide), $C_{10}H_8Cl_6O$. *Cryst. Struct. Comm.* 7:467-471 (1978).
29. Garraway, J. L., and Wain, R. L. The design of auxin-type herbicides. In: *Drug Design*, Vol. 7 (E. J. Ariens, Ed.), Academic Press, New York, 1976, pp. 115-164.
30. Kaethner, T. M. Conformational change theory for auxin structure-activity relationships. *Nature* 267: 19-23 (1977).
31. Kennard, C. H. L., Smith, G., and White, A. H. Structural aspects of phenoxyalkanoic acids. the structure of phenoxyacetic acid, (+)-2-phenoxypropionic acid, (+)-2-(4-chlorophenoxy)propionic acid, 2-methyl-2-phenoxypropionic acid, and 2-(4-chlorophenoxy)-2-methylpropionic acid. *Acta Cryst.* B38: 868-875 (1982).
32. Smith, G., and Kennard, C. H. L. Structural and conformational aspects of phenoxyalkanoic acids as determined in the solid state by diffraction methods. *J. Agr. Food Chem.* 27: 779-787 (1979).
33. Goldstein, J. A. The structure = activity relationships of halogenated biphenyls as enzyme inducers. In: *Health Effects of Halogenated Aromatic Hydrocarbons* (W. J. Nicholson and J. A. Moore, Eds.), New York Academy of Sciences, New York, 1979, pp. 164-178.
34. Poland, A., Greenlee, W. F., and Kende, A. S. Studies on the mechanism of action of the chlorinated dibenzo-*p*-dioxins and related compounds. In: *Health Effects of Halogenated Aromatic Hydrocarbons* (W. J. Nicholson and J. A. Moore, Eds.), New York Academy of Sciences, New York, 1979, pp. 214-230.
35. Poland, A., and Glover, E. Chlorinated biphenyl induction of aryl hydrocarbon hydroxylase activity: a study of the structure-activity relationship. *Mol. Pharmacol.* 13: 924-938 (1977).
36. Poland, A., and Knutson, J. C. 2,3,7,8-Tetrachlorodibenzo-*p*-dioxin and related halogenated aromatic hydrocarbons: examination of the mechanism of toxicity. *Ann. Rev. Pharmacol. Toxicol.* 22: 517-554 (1982).
37. Bandiera, S., Sawyer, T. W., Campbell, M. A., Fujita, T., and Safe, S. Competitive to the cytosolic 2,3,7,8-tetrachlorodibenzo-*p*-dioxin receptor. *Biochem. Pharmacol.* 32: 3803-3813 (1983).
38. McKinney, J. D., Singh, P., Levy, L. A., and Walker, M. P. High toxicity and co-carcinogenic potential of certain halogenated aromatic hydrocarbons—some structure-activity aspects. In: *Safe Handling of Chemical Carcinogens, Mutagens or Tetratogens: Chemists Viewpoint*. (D. Walters, Ed.), Ann Arbor Science Pub., Ann Arbor, MI, 1980, pp. 421-348.

39. McKinney, J. D., and Singh, P. Structure-activity relationships in halogenated biphenyls: unifying hypothesis for structural specificity. *Chem-Biol. Interact.* 33: 271-283 (1981).
40. McKinney, J. D., and McConnell, E. Structural specificity and the dioxin receptor. In: *Chlorinated Dioxins and Related Compounds. Impact on the Environment.* (O. Hutzinger, R. W. Frei, E. Merian, and F. Pocchiarri, Eds.), Pergamon Press, New York, 1982, pp. 367-381.
41. Singh, P., and McKinney, J. D. 2,2',4,4',6,6'-Hexachlorobiphenyl. *Acta Cryst. B35:* 259-262 (1979).
42. Cordes, A. W., and Fair, C. K. Dibenzo-*p*-dioxin. *Acta Cryst. B30:* 1621-1623 (1974).
43. McKinney, J. D., Gottschalk, K. E., and Pedersen, L. A theoretical investigation of the conformation of polychlorinated biphenyls. *J. Mol. Struct.*, 13: 445-450 (1983).
44. Wood, A. W., Chang, R. L., Levin, W., Yagi, H., Thakker, D. R., van Blorderen, P. J., Jerina, D. M., and Conney, A. H. Mutagenicity of the enantiomers of the diastereomeric bay-region benzo(a)anthracene 3,4-diol-1,2-epoxides in bacterial and mammalian cells. *Cancer Res.* 43: 5821-5825 (1983).
45. Phillips, D. H. Fifty years of benzo(a)pyrene. *Nature* 303: 468-472 (1983).
46. Glusker, J. P. Structural aspects of steroid hormones and carcinogenic polycyclic aromatic hydrocarbons. In: *Biochemical Actions of Hormones, Vol. IV*, Academic Press, New York, 1979, pp. 121-204.
47. Kashino, S., Zacharias, D. E., Prout, C. K., Carrell, H. L., Glusker, J. P., Hecht, S. S., and Harvey, R. S. Structure of 5-methylchripene, C₁₉H₁₄. *Acta Cryst. C40:* 536-540 (1984).
48. Glusker, J. P., Zacharias, D. E., Whalen, D. L., Friedman, S., and Pohl, T. M. Internal hydrogen bond formation in a *syn*-hydroxyepoxide. *Science* 215: 695-696 (1982).
49. Klein, C. L., Majeste, R. J., Tsang, W. S., Griffin, G. W., and Stevens, E. D. Structure of *cis*-2,3-tetraindiol, *cis*-1,2,3,4-tetrahydro-2,3-naphthalenediol, C₁₀H₁₂O₂. *Acta Cryst. C39:* 1405-1407 (1983).
50. Klein, C. L., and Stevens, E. D. Structure of *syn*-3,4-dimethoxy-1,2-epoxy-1,2,3,4-tetrahydronaphthalene, C₁₂H₁₄O₃. *Acta Cryst. C40:* 315-317 (1984).
51. Klein, C. L., and Stevens, E. D. Molecular structure of *anti*-3,4-dihydroxy-1,2,3,4-tetrahydronaphthalene-1,2-oxide. *Cancer. Res.* 44: 1523-1526 (1984).
52. Neidle, S., Subbiah, A., Cooper, C. S., and Riberio, O. Molecular structure of (+)7 α -8 β -dihydroxy-9 β ,10 β -epoxy-7,8,9,10-tetrahydrobenzo(a)pyrene; an X-ray crystallographic study. *Carcinogenesis* 1: 249-254 (1980).
53. Klopman, G., Grinberg, H., and Hopfinger, A. J. MINDO/3 calculations of the conformation and carcinogenicity of epoxy-metabolites of aromatic hydrocarbons; 7,8-dihydroxy-9,10-epoxy-7,8,9,10-tetrahydrobenzo(a)pyrene. *J. Theor. Biol.* 79: 355-366 (1979).
54. Mohammad, S. N., Hopfinger, A. J., and Bickers, D. R. Intrinsic mutagenicity of polycyclic aromatic hydrocarbons: a quantitative structure activity study based upon molecular shape analysis. *J. Theor. Biol.* 102: 323-331 (1983).
55. Hitchings, G. H., and Burchall, J. J. Inhibition of folate biosynthesis and function as a basis for chemotherapy. *Adv. Enzymol.* 27: 417-468 (1965).
56. Zakrzewski, S. F., Dave, C., and Rosen, F. Comparison of the antitumor activity and toxicity of 2,4-diamino-5-(1-adamantyl)-6-methylpyrimidine and 2,4-diamino-5-(1-adamantyl)-6-ethylpyrimidine. *J. Natl. Cancer Inst.* 60: 1029-1033 (1978).
57. Cody, V., and Zakrzewski, S. F. Molecular structure of 2,4-diaminopyrimidine antifolates with antineoplastic activity. *J. Med. Chem.* 25: 427-430 (1982).
58. Cody, V., DeJarnette, E., and Zakrzewski, S. F. Structure-activity relationships among 5-substituted lipophilic diaminopyrimidine antineoplastic antifolates. In: *Chemistry and Biology of Pteridines* (J. A. Blair, Ed.), Walter de Gruyter & Co., Berlin, 1983, pp. 293-297.
59. Cody, V. Structures of two active trimethoprim analogues: 2,4-diamino-5-(4-isopropenyl-5-dimethoxybenzyl)pyrimidium ethanesulfonate, C₁₆H₂₁N₃O₂⁺·C₂H₅O₃S⁻ (I), and 2,4-diamino-5-(3,5-dimethoxy-4-methoxycarbonylbenzyl)pyrimidine, C₁₅H₁₈N₃O₄ (II). *Acta Cryst. C40:* 1000-1004 (1984).
60. Koetzle, T. F., and Williams, G. J. B. The crystal and molecular structure of the antifolate drug trimethoprim (2,4-diamino-5-(3',4',5'-trimethoxybenzyl)pyrimidine. A neutron diffraction study. *J. Am. Chem. Soc.* 98: 2075-2078 (1976).
61. Camerman, A., Smith, H. W., and Camerman, N. Stereochemistry of dihydrofolate reductase inhibitor antitumor agents: molecular structure of 'Baker's antifol' (triazinate) and 'insoluble Baker's antifol'. *Acta Cryst. B35:* 2113-2118 (1979).
62. Fontecilla-Camps, J. C., Bugg, C. E., Temple, C. Jr., Rose, J. D., Montgomery, J. A., and Kisluk, R. L. Absolute configuration of biological tetrahydrofolates. A crystallographic determination. *J. Am. Chem. Soc.* 101: 6114-6115 (1979).
63. Mastropaola, D., Camerman, A., and Camerman, N. Folic acid. Crystal structure and implications for enzyme binding. *Science* 210: 334-336 (1980).
64. Welsh, W. J., Cody, V., Mark, J. E., and Zakrzewski, S. F. CNDO/2 molecular orbital calculations on the antifolate DAMP and some related species: structural geometries, ring distortions, charge distributions and conformational characteristics. *Cancer Biochem. Biophys.* 7: 27-38 (1983).
65. Bolin, J. T., Filman, D. J., Matthews, D. A., Hamlin, R. C., and Kraut, J. Crystal structures of *E. coli* and *L. casei* dihydrofolate reductase refined at 1.7Å resolution. *J. Biol. Chem.* 257: 13650-13662 (1982).
66. Spark, M. J., Winkler, D. A., and Andrews, P. R. Conformational analysis of folates and folate analogues. *Inter. J. Quant. Chem. Quant. Biol. Symp.* 9: 321-334 (1982).
67. Dauber, P., Osguthrope, D. J., and Hagler, A. T. Structure, energetics, and dynamics of ligand binding to dihydrofolate reductase. *Biochem. Soc. Trans.* 10: 312-318 (1982).
68. Cody, V. Thyroid hormone interactions: molecular conformation, protein binding, and hormone action. *Endocrine Rev.* 1: 140-166 (1980).
69. Okabe, N., Fujiwara, T., Yamagata, Y., and Tomita, K. The crystal structure of a major metabolite of thyroid hormone: 3,3',5'-triiodo-L-thyronine. *Biochim. Biophys. Acta* 717: 179-181 (1982).
70. Cody, V., and Murray-Rust, P. Iodine...X(O,N,S) intermolecular contacts: models of thyroid hormone-protein binding interactions using information from the Cambridge crystallographic data files. *J. Mol. Struct.* 112: 189-199 (1984).
71. Fekkes, D., Hennemann, G., and Visser, T. J. One enzyme for the 5'-deiodination of 3,3',5'-triiodothyronine and 3',5'-diiodothyronine in rat liver. *Biochem. Pharmacol.* 31: 1705-1709 (1982).
72. Aufmkolk, M., Kohrle, J., and Rokos, H. Structure-function relationships of iodothyronine analogs inhibiting iodothyronine deiodinase. *Ann. Endocrin.* 43: 85A (1982).
73. Wu, S.-Y., Chopra, I. J., Solomon, D. H., and Johnson, D. E. The effect of repeated administration of ipodate (Oragrafin) in hyperthyroidism. *J. Clin. Endocrinol. Metab.* 47: 1358-1362 (1978).
74. Aufmkolk, M., Kohrle, J., Moore, M., and Hesch, R. D. Aurones—potent inhibitors of iodothyronine deiodinase. *Ann. Endocrin.* 44: 61A (1983).
75. Cody, V., and Aufmkolk, M. Computer graphic analysis of thyroid hormone deiodinase inhibitor structure-activity relationships. *Ann. Endocrin.* 44: 61A (1983).
76. Volz, K. W., Matthews, D. A., Alden, R. A., Freer, S. T., Hansch, C., Kaufman, B. T., and Kraut, J. Crystal structure of avian dihydrofolate reductase containing phenyltriazine and NADPH. *J. Biol. Chem.* 257: 2528-2536 (1982).
77. Blake, C. C. F. Prealbumin and thyroid hormone nuclear receptor. *Proc. Roy. Soc. London B211:* 413-431 (1981).
78. McKinney, J. D., Chae, K., Oatley, S., and Blake, C. C. F. Molecular interactions of toxic chlorinated dibenzo-*p*-dioxins and dibenzofurans with thyroxine binding prealbumin. *J. Med. Chem.* 28: 375-380 (1985).